Binary Neutron Stars: Mergers, Kilonovae, and Their Host Galaxies

Youjun Lu

National Astronomical Observatories of China

School of Astronomy and Space Sciences-University of Chinese Academy of Sciences

Collaborators:
Qingbo Chu, Chunyang Zhao, Hao Ma, Shenghua Yu, Zhiwei Chen, Siqi Zhang……

Outline

- Background: current status of BNS observations
- Formation and Evolution of BNSs
- Distribution, merger rate, and properties of BNSs
- Electromagnetic counterparts of BNS mergers: kilonovae
- Detection rate of kilonova
- Prospects
- Summary

Neutron Stars

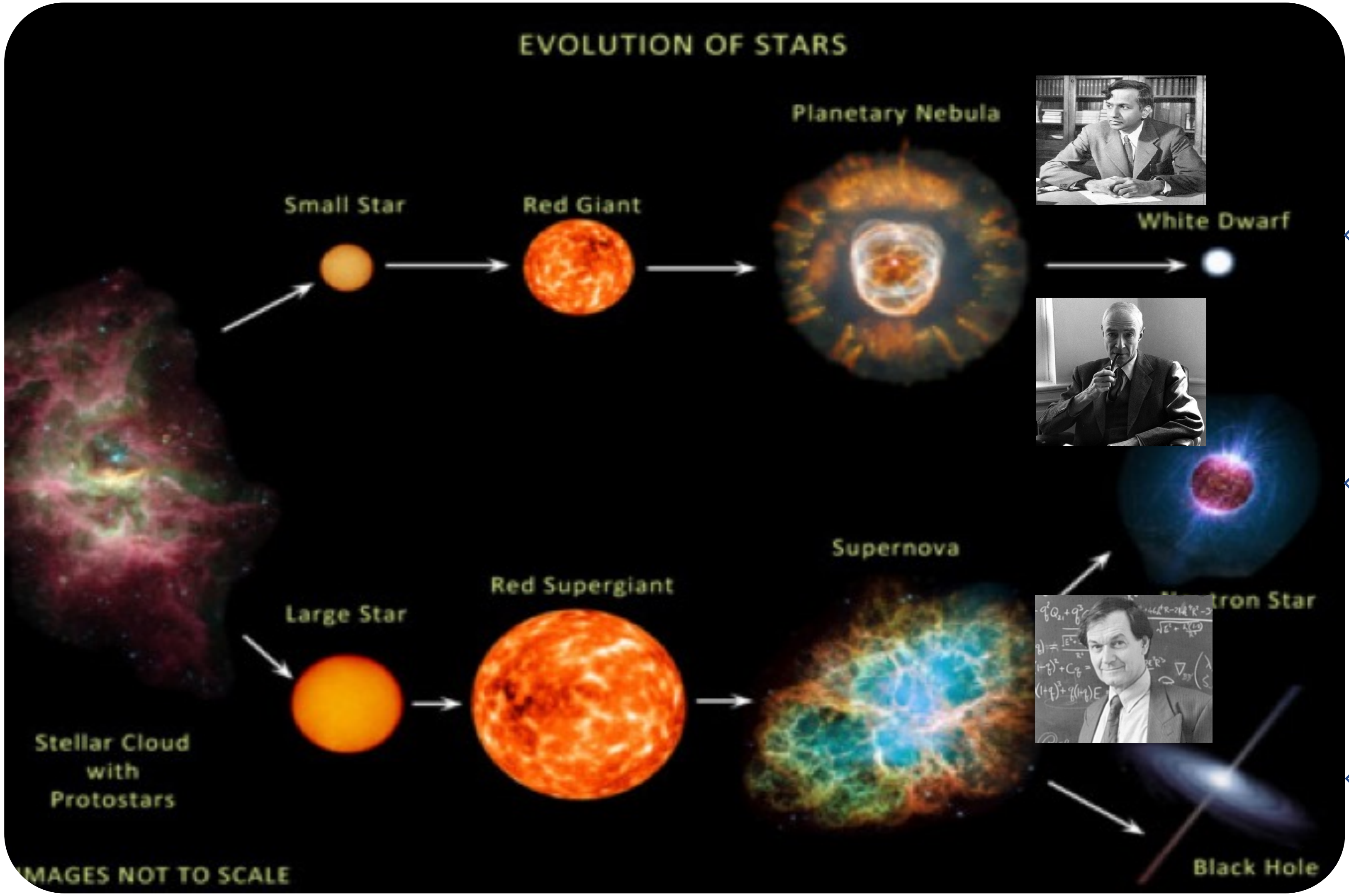

Initial Mass

$<9M_{\odot}$
Electron degeneracy pressure
→white dwarfs

$\sim 9\text{-}25M_{\odot}$
Neutron degeneracy pressure
→Neutron stars

$>25M_{\odot}$
No known physics
→Black Holes

Neutron Stars

Pulsar discovery:

✓PSR B1919+21: 1.4$M_\odot$, P=1.3373s (1968.11.28);

✓>3000 pulsars (FAST +++)

✓Extremely massive one 2.14$M_\odot$ Cromartie+ 2020, Nat Astro.

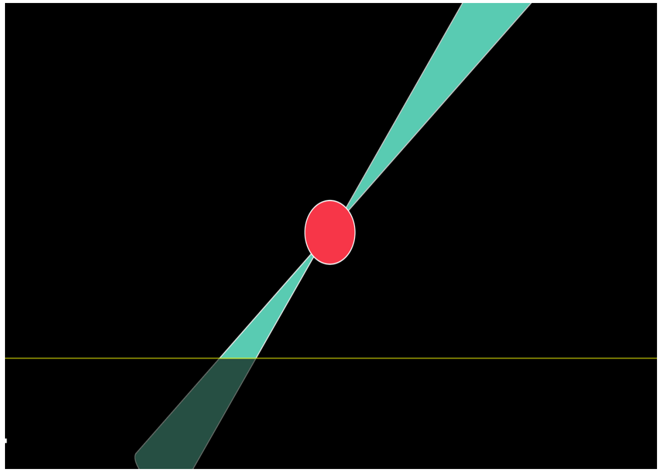

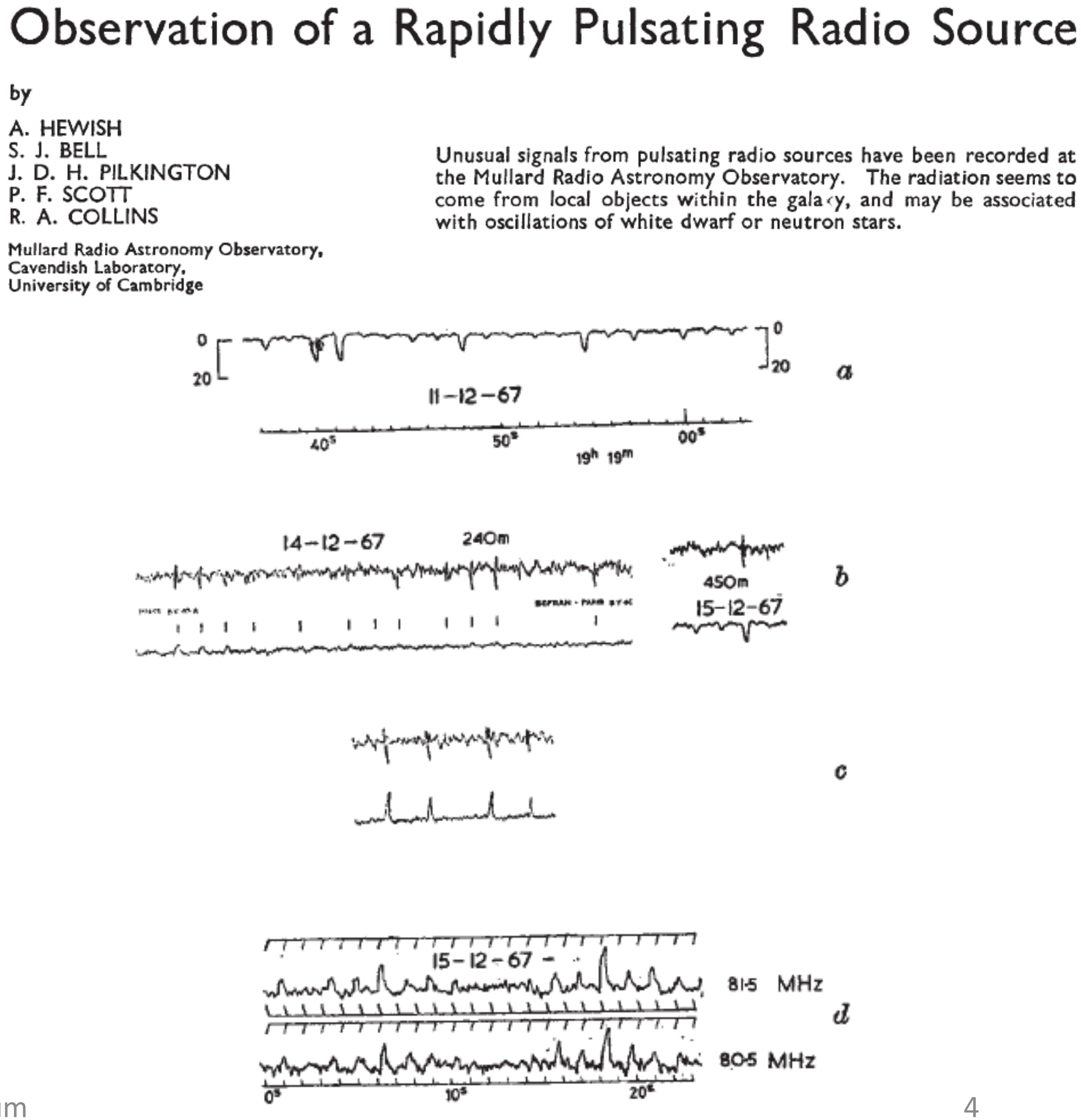

Observation of a Rapidly Pulsating Radio Source

by
A. HEWISH
S. J. BELL
J. D. H. PILKINGTON
P. F. SCOTT
R. A. COLLINS

Mullard Radio Astronomy Observatory, Cavendish Laboratory, University of Cambridge

Unusual signals from pulsating radio sources have been recorded at the Mullard Radio Astronomy Observatory. The radiation seems to come from local objects within the galaxy, and may be associated with oscillations of white dwarf or neutron stars.

Binary Neutron Stars (BNSs)

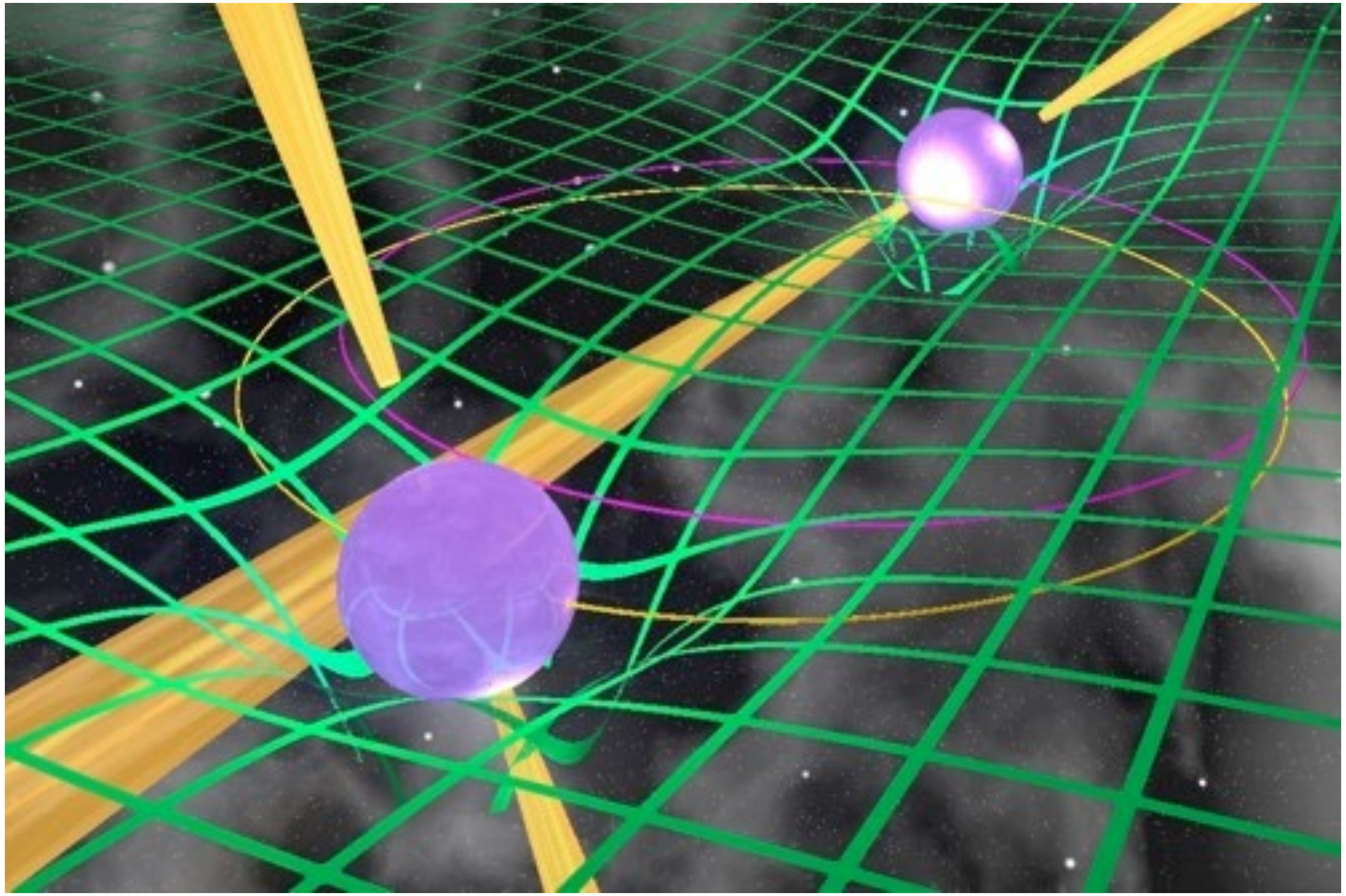

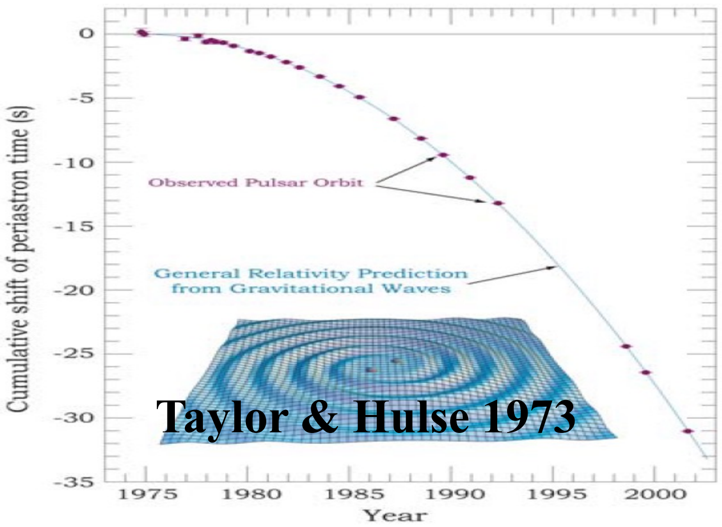

Binary Neutron Stars/pulsasrs：

✓PSR J0737-3039: $1.337M_{\odot}+1.250M_{\odot}$, 23ms+2.8s; Period=2.8hrs

✓PSR B1913+16: $1.387M_{\odot}+1.441M_{\odot}$, 59ms+Neutron star; Period=7.75hrs

Binary Neutron Stars: Galactic BNSs

System	$P_{\rm orb}$ [day]	e	$M_{\rm psr}$ [$M_\odot$]	$M_{\rm comp}$ [$M_\odot$]	$M_{\rm total}$ [$M_\odot$]	mass ratio	$\tau_{\rm GW}$ [10^{10} yr]	Reference
				Milky Way field				
J0737−3039	0.102	0.088	1.338	1.249	2.587	0.93	0.0086	Tauris et al. (2017)
B1534+12	0.421	0.274	1.333	1.346	2.678	0.99	0.27	Tauris et al. (2017)
J1756−2251	0.320	0.181	1.341	1.230	2.570	0.92	0.17	Tauris et al. (2017)
J1906+0746⋆	0.166	0.085	1.291	1.322	2.613	0.98	0.031	Tauris et al. (2017)
J1913+1102	0.206	0.090	1.62	1.27	2.88	0.78	0.047	Ferdman et al. (2020)
J1946+2052	0.078	0.064	<1.31	>1.18	2.50	-	0.0047 – 0.0049$^\Delta$	Stovall et al. (2018)
J0453+1559	4.072	0.113	1.559	1.174	2.734	0.75	150	Tauris et al. (2017)
J1411+2551	2.616	0.170	<1.62	>0.92	2.538	-	49-51$^\Delta$	Martinez et al. (2017)
J1518+4904	8.634	0.249	1.41	1.31	2.718	0.93	920	Tauris et al. (2017)
J1753−2240	13.638	0.304	-	-	-	-	-	Tauris et al. (2017)
J1755−2550⋆	9.696	0.089	-	>0.40	-	-	-	Tauris et al. (2017)
J1811−1736	18.779	0.828	<1.64	>0.93	2.57	-	181-187$^\Delta$	Tauris et al. (2017)
J1829+2456	1.176	0.139	<1.38	>1.22	2.59	-	5.9-6.1$^\Delta$	Tauris et al. (2017)
J1930−1852	45.060	0.399	<1.32	>1.30	2.59	-	55400-57200$^\Delta$	Tauris et al. (2017)
J0509+3801	0.380	0.586	1.34	1.46	2.805	0.92	0.058	Lynch et al. (2018)
J1757−1854	0.184	0.606	1.338	1.395	2.733	0.96	0.0076	Cameron et al. (2018)
B1913+16	0.323	0.617	1.440	1.389	2.828	0.97	0.030	Tauris et al. (2017)
				Milky Way Globular Cluster				
B2127+11C	0.335	0.681	1.358	1.354	2.713	0.997	0.022	Tauris et al. (2017)
J1807−2500⋆	9.957	0.747	1.366	1.206	2.572	0.88	110	Tauris et al. (2017)
J0514−4002⋆	18.8	0.89	1.25	1.22	2.473	0.98	47	Ridolfi et al. (2019)

Laser Interferometer GW Observatories: BNS mergers

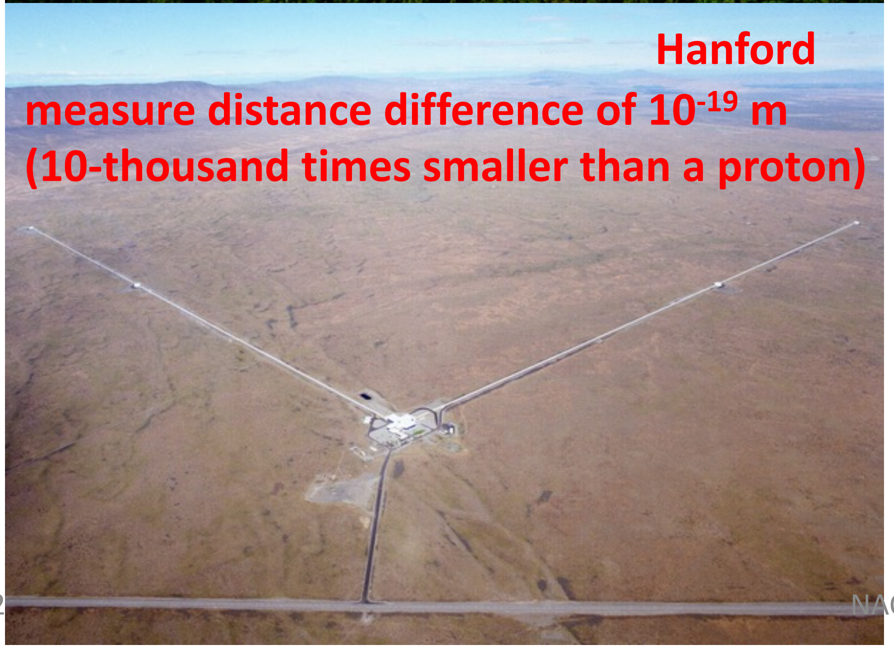

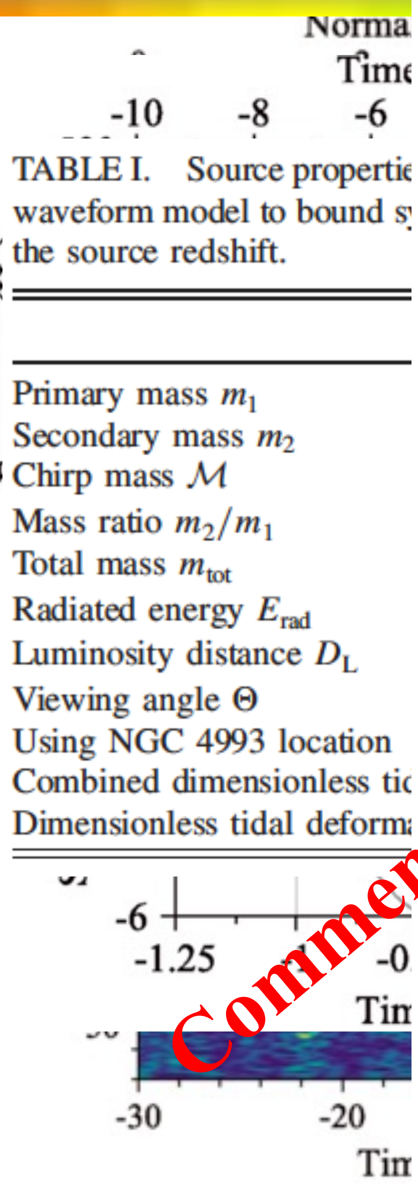

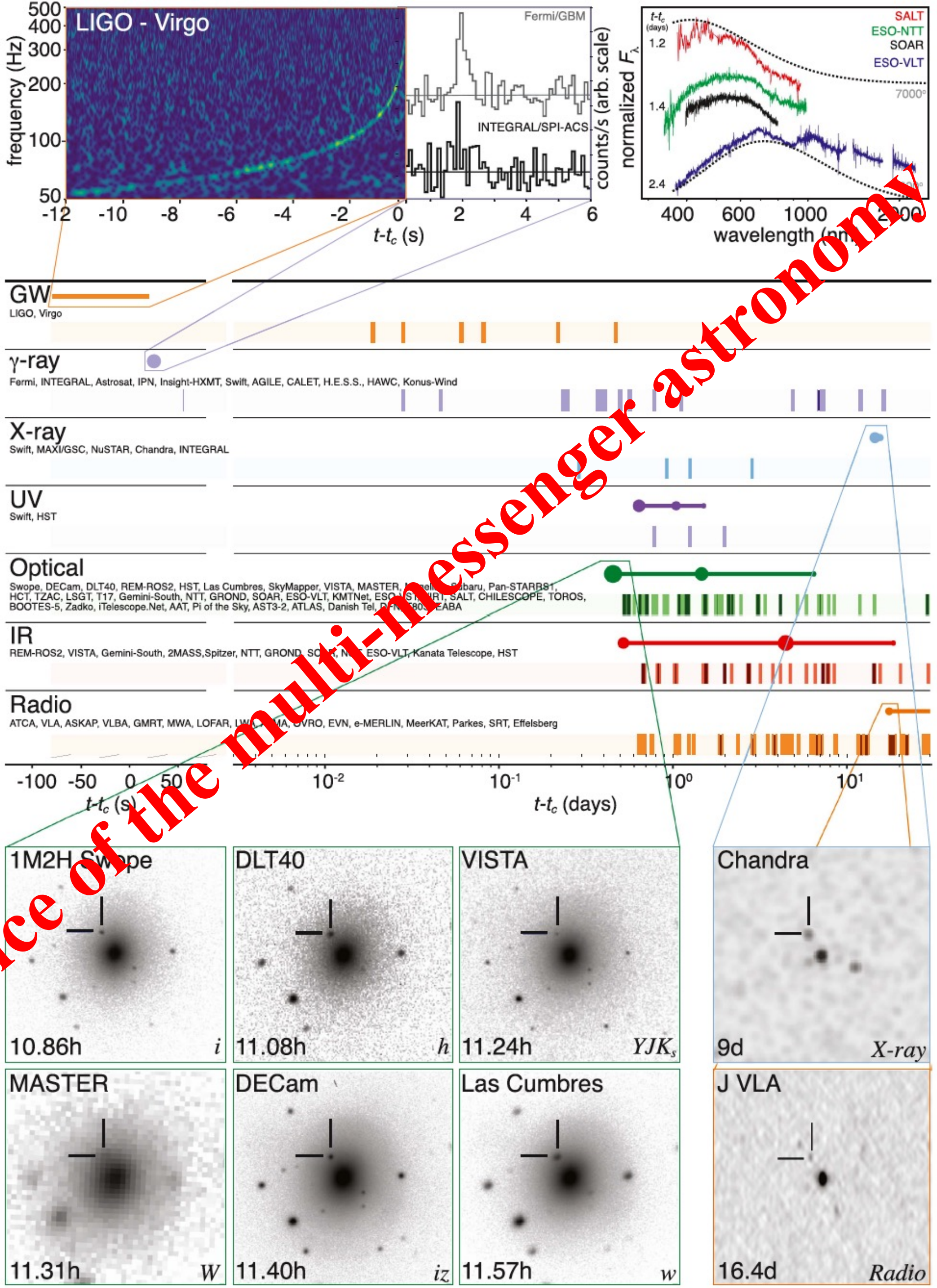

Commence of the multi-messenger astronomy

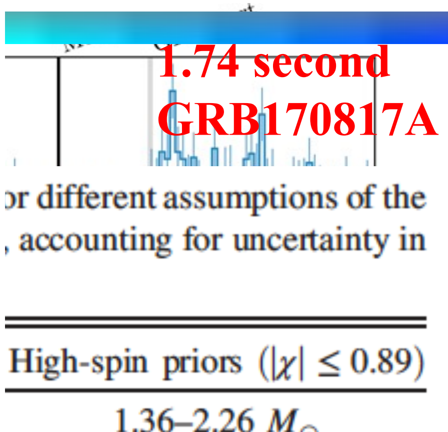

1.74 second
GRB170817A

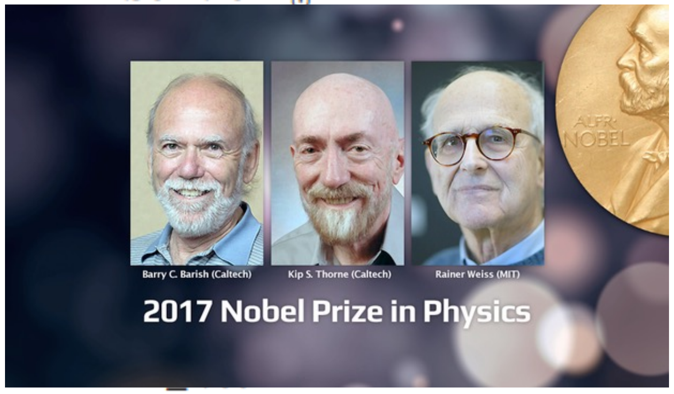

GW170817: kilonova

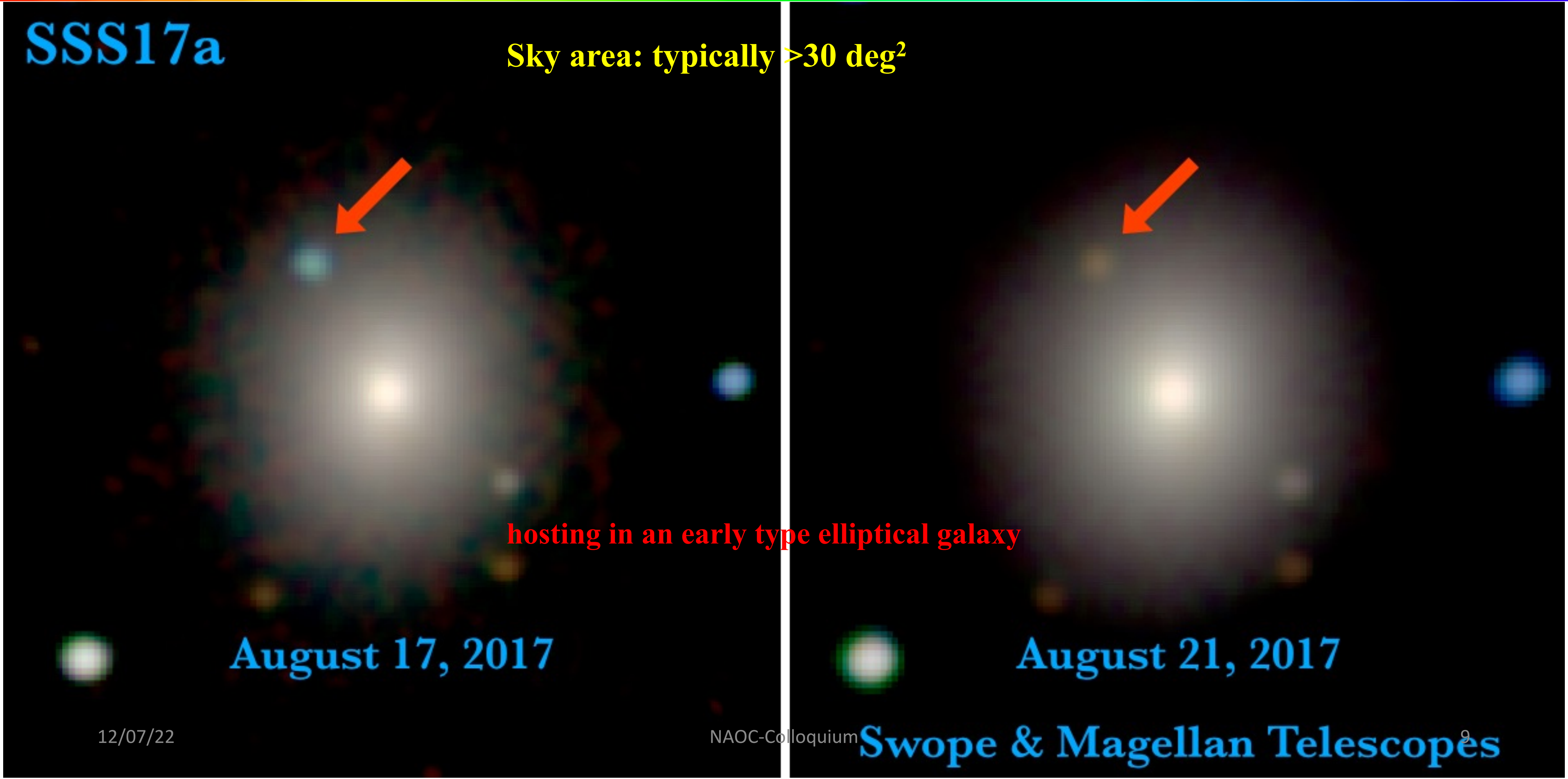

Sky area: typically >30 deg^2

hosting in an early type elliptical galaxy

BNS mergers: GW190425

Sky area: typically >30 deg^2

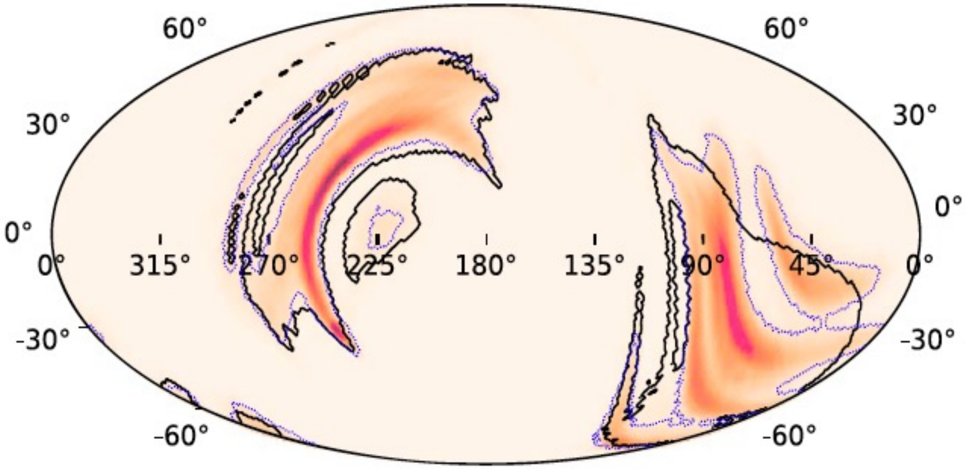

Source Properties for GW190425

	Low-spin Prior ($\chi < 0.05$)	High-spin Prior ($\chi < 0.89$)
Primary mass m_1	1.60–1.87 $M_\odot$	1.61–2.52 $M_\odot$
Secondary mass m_2	1.46–1.69 $M_\odot$	1.12–1.68 $M_\odot$
Chirp mass $\mathcal{M}$	$1.44^{+0.02}_{-0.02}$ $M_\odot$	$1.44^{+0.02}_{-0.02}$ $M_\odot$
Detector-frame chirp mass	$1.4868^{+0.0003}_{-0.0003}$ $M_\odot$	$1.4873^{+0.0008}_{-0.0006}$ $M_\odot$
Mass ratio m_2/m_1	0.8 – 1.0	0.4 – 1.0
Total mass m_{tot}	$3.3^{+0.1}_{-0.1}$ $M_\odot$	$3.4^{+0.3}_{-0.1} M_\odot$
Effective inspiral spin parameter χ_{eff}	$0.012^{+0.01}_{-0.01}$	$0.058^{+0.11}_{-0.05}$
Luminosity distance D_L	159^{+69}_{-72} Mpc	159^{+69}_{-71} Mpc
Combined dimensionless tidal deformability $\tilde{\Lambda}$	$\leqslant 600$	$\leqslant 1100$

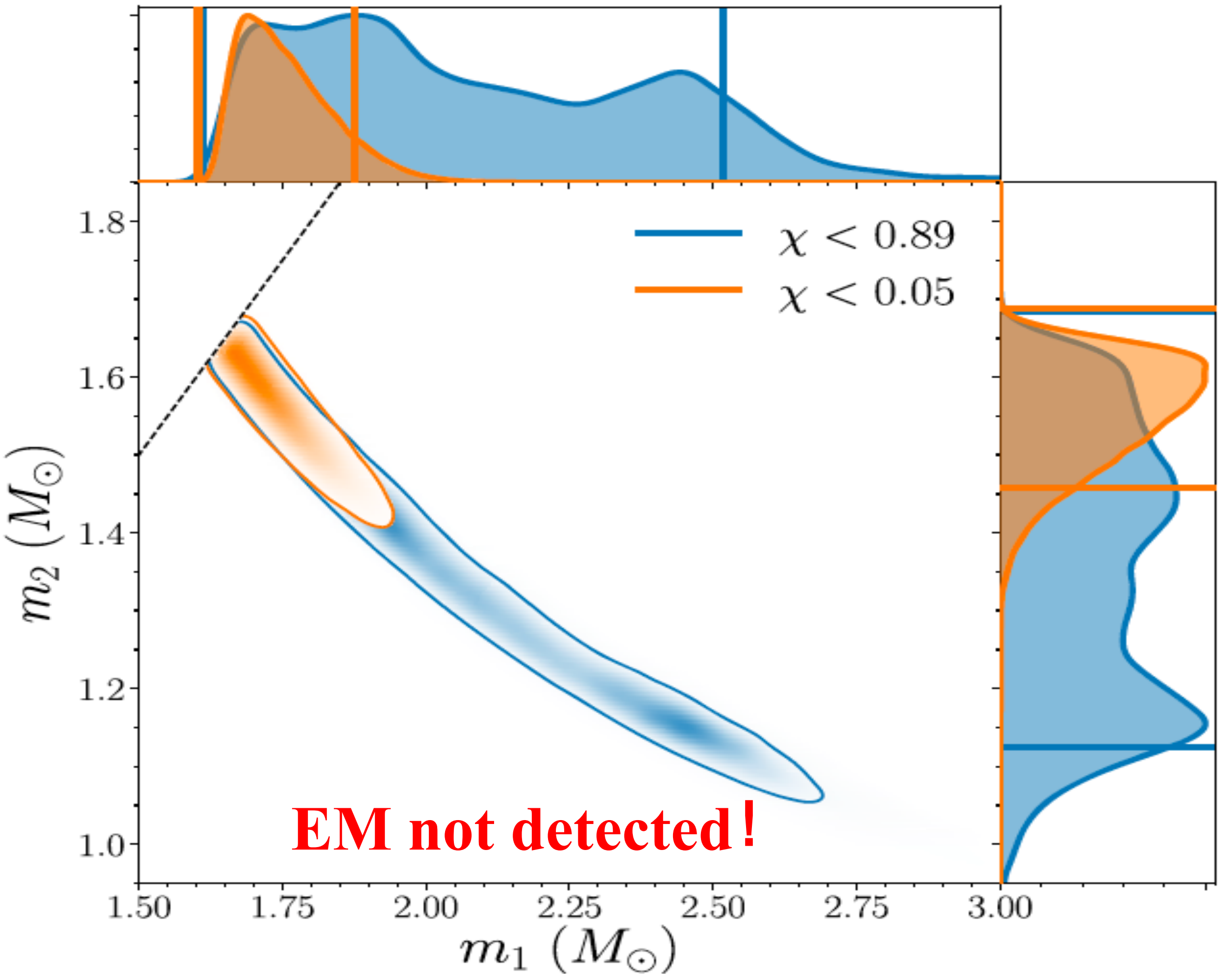

EM not detected!

BNS mergers

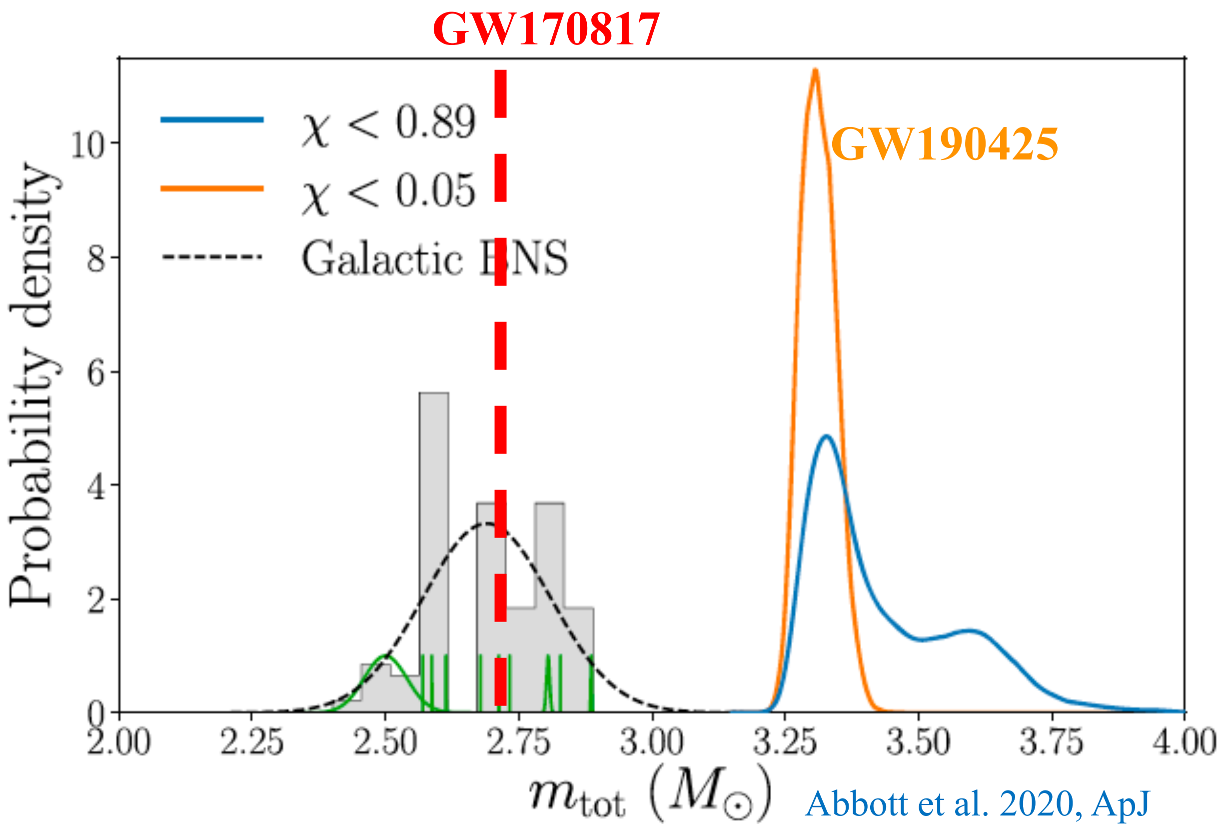

Abbott et al. 2020, ApJ

Abbott et al. arXiv:2111.03634

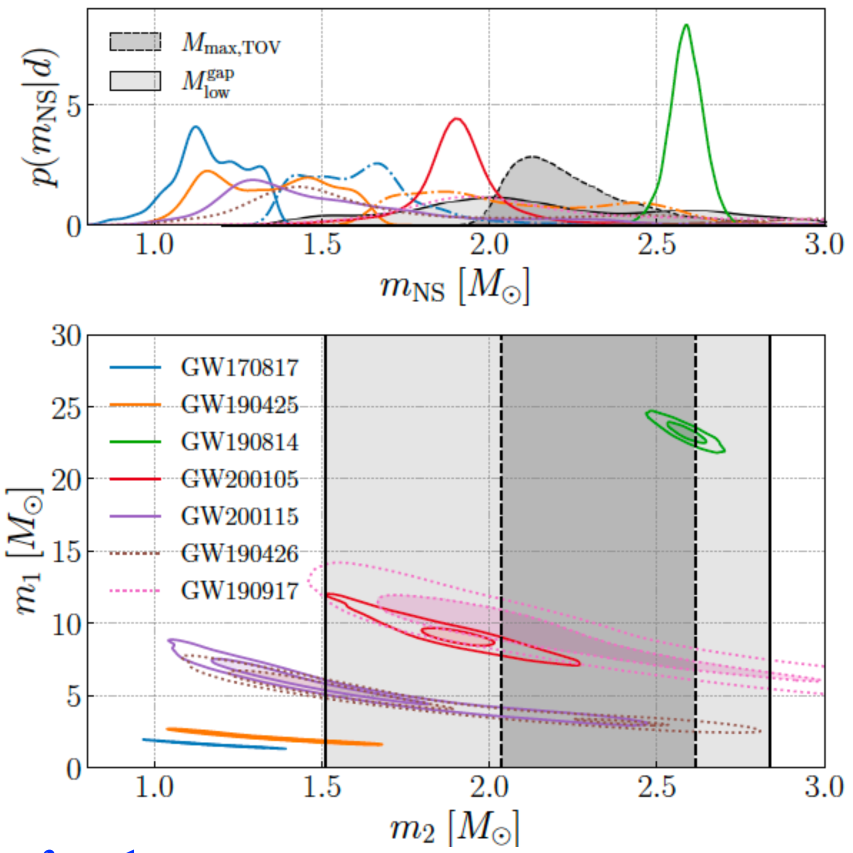

Merger rate: 10-1700 Gpc^{-3} yr^{-1}
M_{TOV}: ~2-2.5$M_\odot$
Total mass distribution: any tension?

LIGO-Virgo-KAGRA and future GW observations

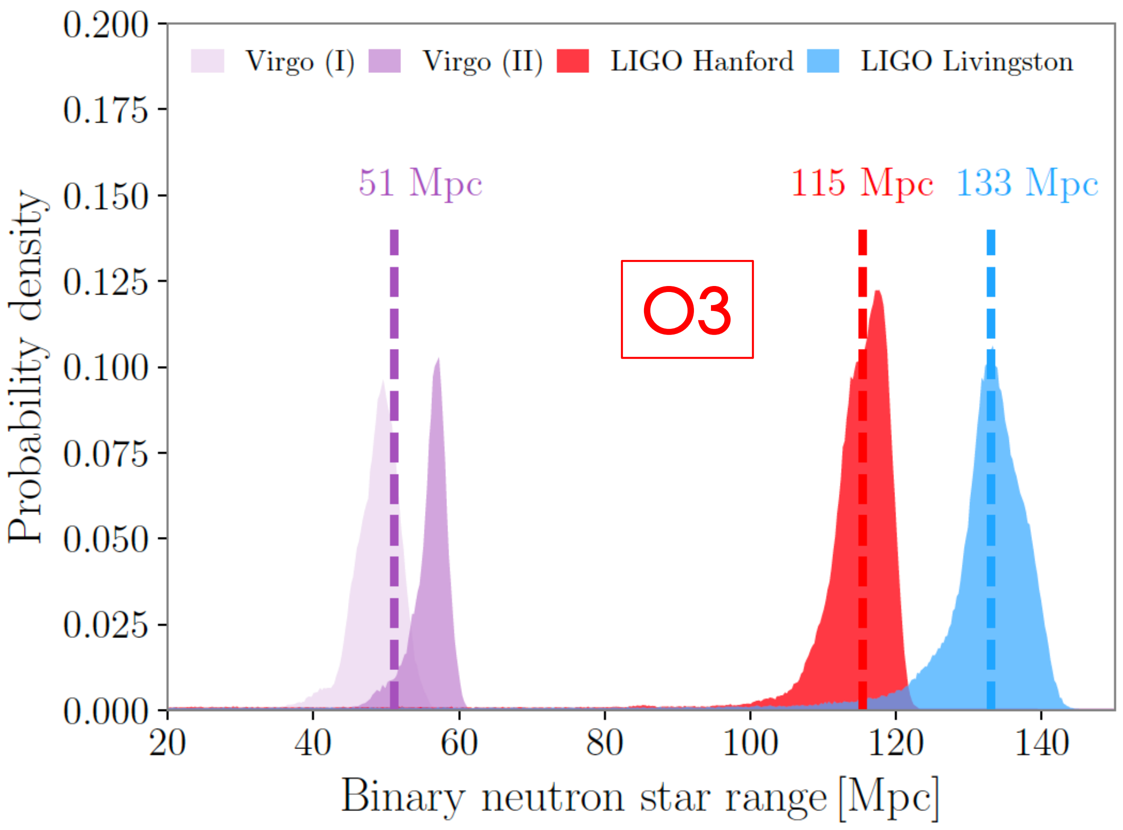

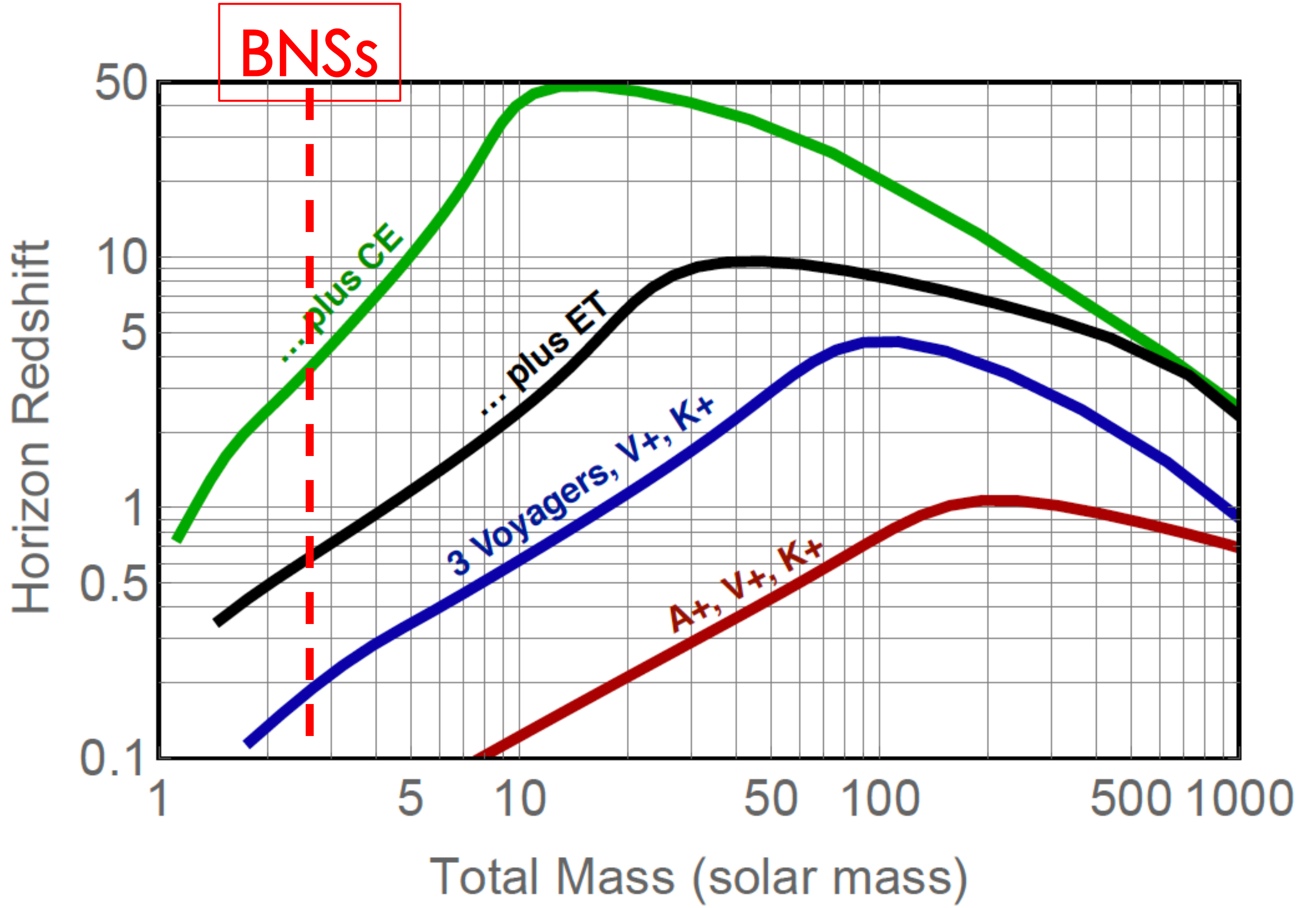

Many more BNS mergers are expected to be detected by GW detectors.
LIGO A+: >several tens; LIGO Voyagers: >several hundreds; ET: ~10^4; CE: ~10^5;
LIGO-Virgo-KAGRA O4: a few or more? (2023.03-)

Important Questions

- How did BNSs form in the universe?
- How are the BNSs distributed in the universe?
- How do the EM signals depend on the properties of progenitor BNSs?
- How to search and detect kilonovae?
- What are the host galaxies of BNS mergers?
- How to constrain the EOS of neutron stars according to the multi-messenger information?
- What are the remnant of BNS mergers?
- ……

Models for BNSs: key ingredients

- ✧Binary star evolution (or dynamical origin?)
- ✧Orbital evolution of BNSs
- ✧Star formation and metallicity enrichment history of each galaxy
- ✧Formation and evolution of galaxies in the universe
- ✧Mergers of BNSs (relativistic) dynamical processes
- ✧kilonova model (detailed microphysics for radiation)
- ✧……

Binary Star Evolution

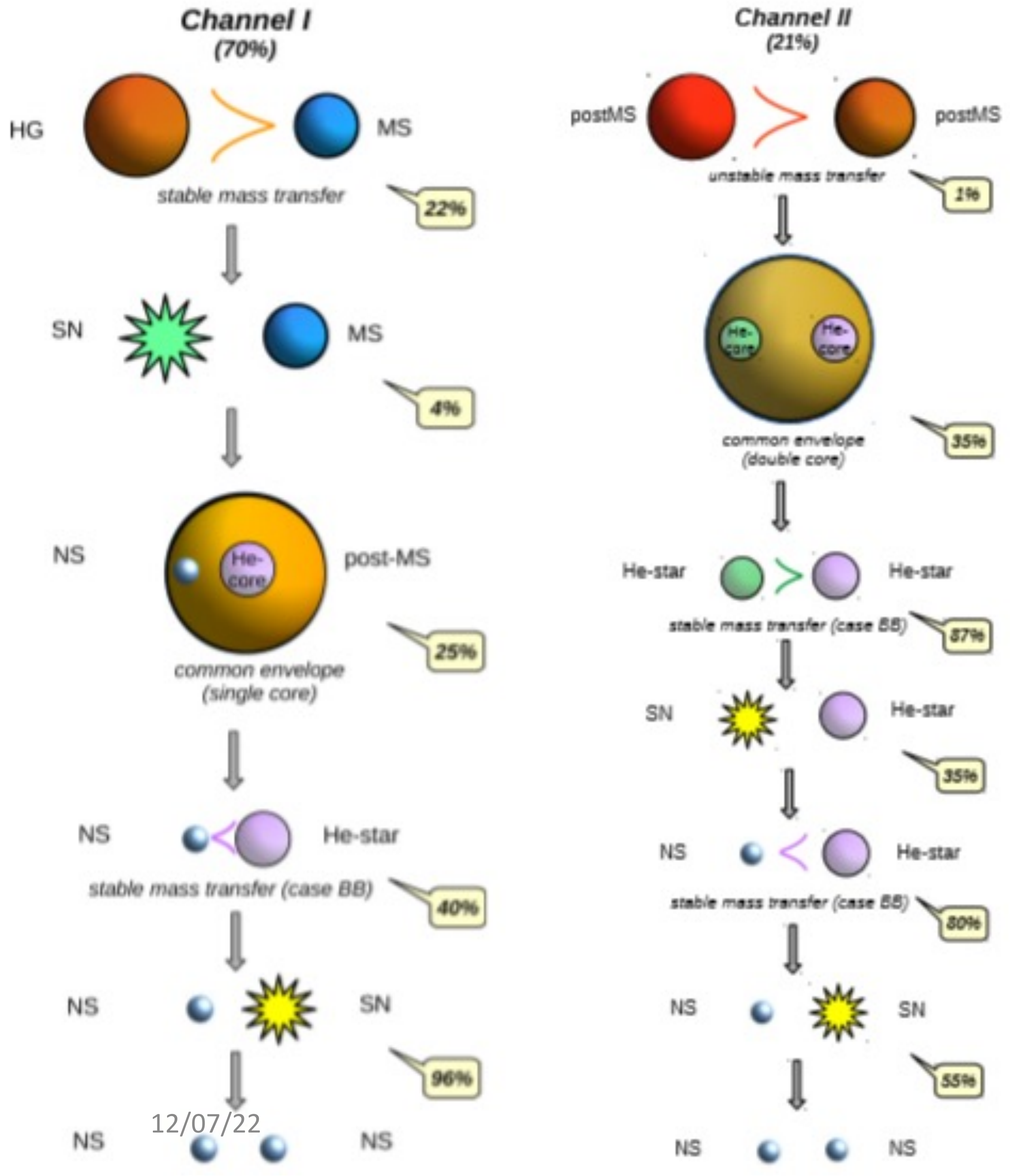

Heirachival Galaxy formation

EAGLE Simulation

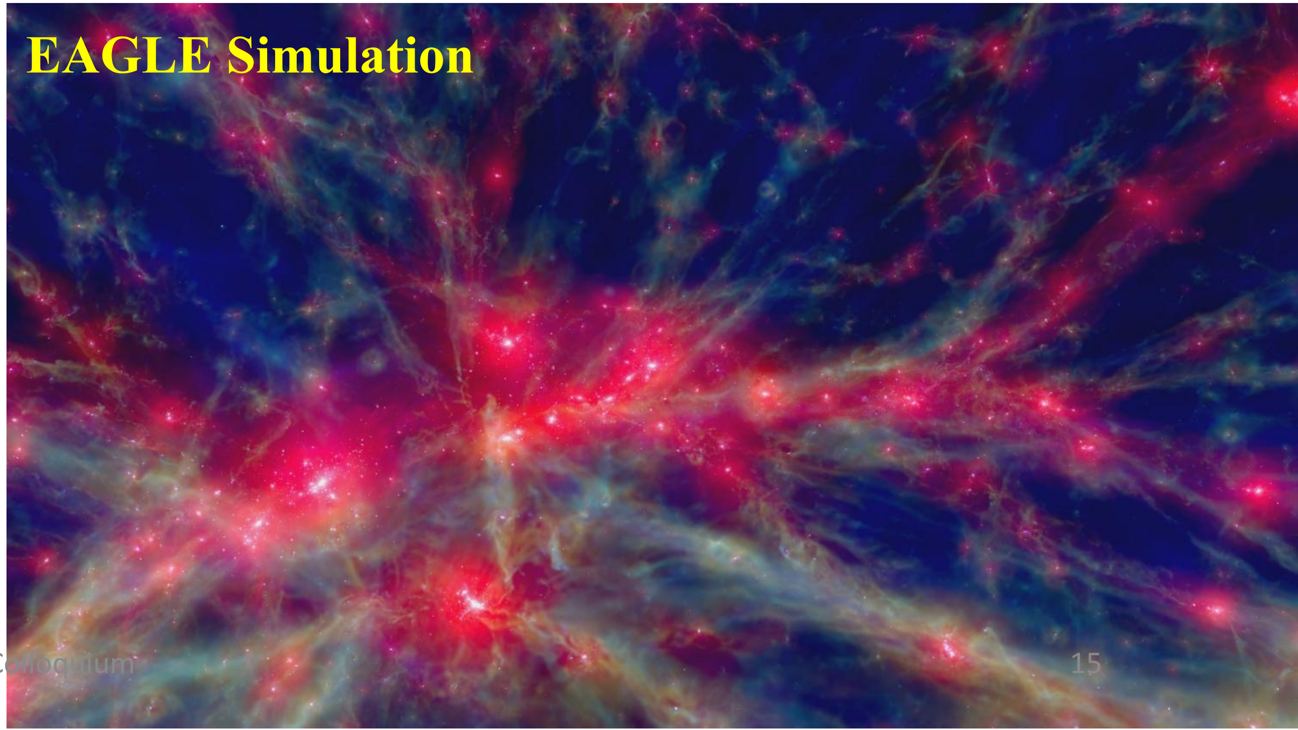

Population Synthesis Models for Formation of BNSs

- Common Envelope Evolution (CE)
  - α-formalism $$\frac{G(m_1 - m_{1c})m_1}{\lambda r_L} = \alpha_{CE}\left(\frac{Gm_{1c}m_2}{2a_f} - \frac{Gm_1m_2}{2a_i}\right),$$
  - γ-formalism $$\frac{J_i - J_f}{J_i} = \gamma\frac{m_1 - m_{1c}}{m_1 + m_2},$$
- Kick velocity

$$\frac{dN}{N dv_k} = \left(\frac{2}{\pi}\right)^{1/2} \frac{v_k^2}{\sigma_k^3} \exp^{-v_k^2/2\sigma_k^2},$$

- Mass ejection

$$\beta = \frac{M_{NS} + M_2}{M_{He} + M_2},$$

- Formation route for BNSs

(a) CE ejection + CE ejection;
(b) Stable RLOF + CE ejection;
(c) CE ejection + stable RLOF;
(d) Stable RLOF + stable RLOF
(e) Exposed core + CE ejection;
(f) Solo CE ejection;
(g) Solo RLOF.

- Remnant mass

$$m_{NS} = 0.89 + 0.23 m_{c,SN}$$

Stiff EOS

Or mass relation given by Spera et al. 2015

Model	$\alpha\lambda$ or γ	σ_k [km s^{-1}]
α0.1kl	$\alpha\lambda = 0.05$	30
α0.1kh	$\alpha\lambda = 0.05$	190
α0.1kb	$\alpha\lambda = 0.05$	190/30
α1.0kl	$\alpha\lambda = 0.5$	30
α1.0kh	$\alpha\lambda = 0.5$	190
α1.0kb	$\alpha\lambda = 0.5$	190/30
α10.kl	$\alpha\lambda = 5.0$	30
α10.kh	$\alpha\lambda = 5.0$	190
α10.kb	$\alpha\lambda = 5.0$	190/30
γ1.1kl	$\gamma = 1.1$	30
γ1.1kh	$\gamma = 1.1$	190
γ1.1kb	$\gamma = 1.1$	190/30
γ1.3kl	$\gamma = 1.3$	30
γ1.3kh	$\gamma = 1.3$	190
γ1.3kb	$\gamma = 1.3$	190/30
γ1.5kl	$\gamma = 1.5$	30
γ1.5kh	$\gamma = 1.5$	190
γ1.5kb	$\gamma = 1.5$	190/30
γ1.7kl	$\gamma = 1.7$	30
γ1.7kh	$\gamma = 1.7$	190
γ1.7kb	$\gamma = 1.7$	190/30

Chu et al. 2022, MNRAS

Formation and evolution of BNSs

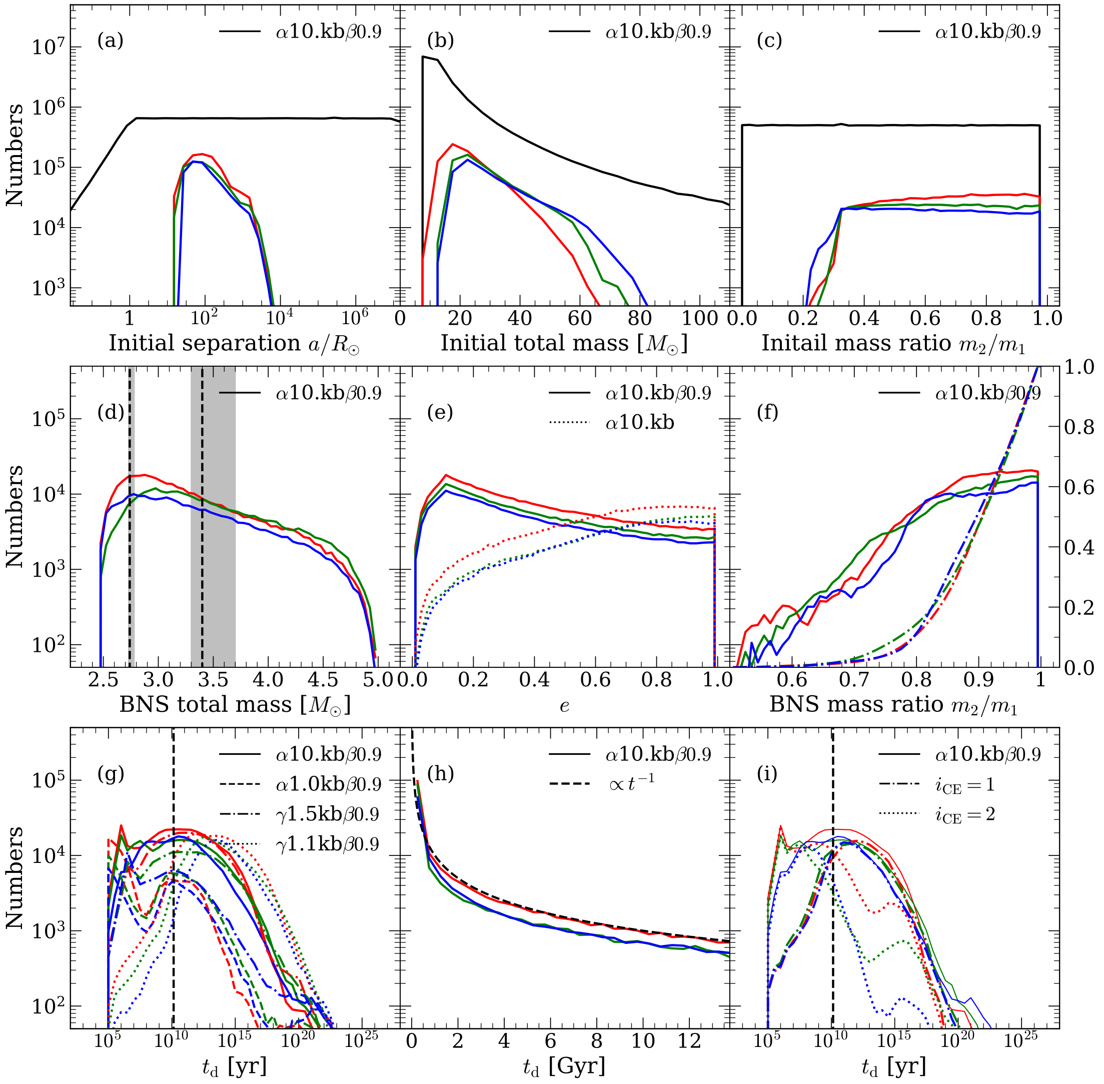

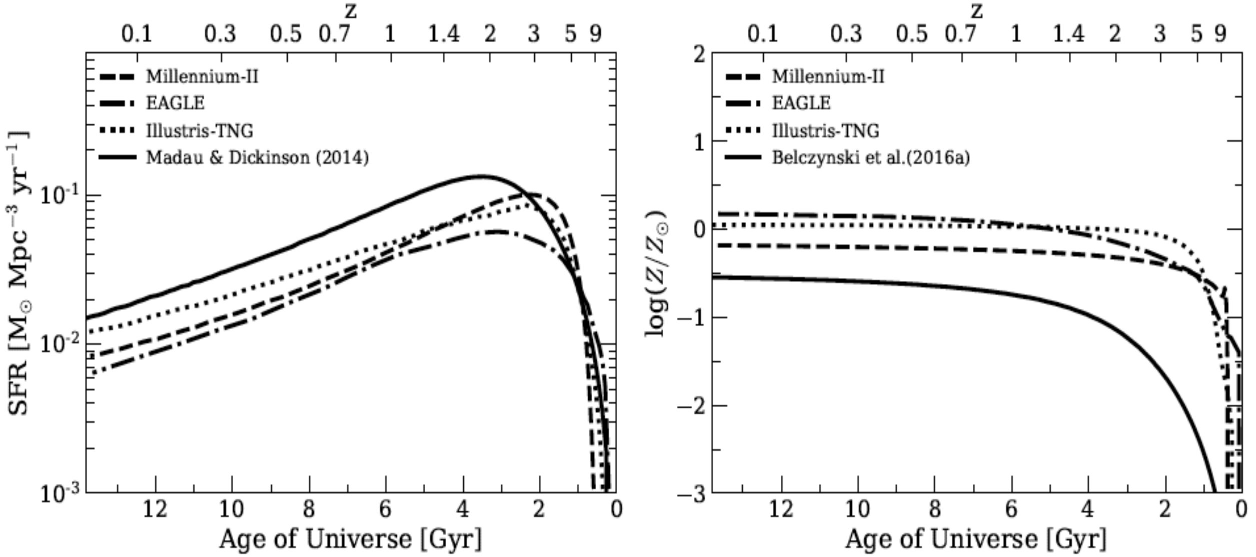

Population synthesis：

- ➢ **Common evenlope evolution**
- ➢ **Kick velocity**
- ➢ **Mass ejection**
- ➢ **Remnant mass**

Galaxy formation and evolution in the universe:
Millennium-II, EAGLE, Illustris-TNG，
Observational SFR/metallicity history

Chu et al. 2022

Galactic BNSs

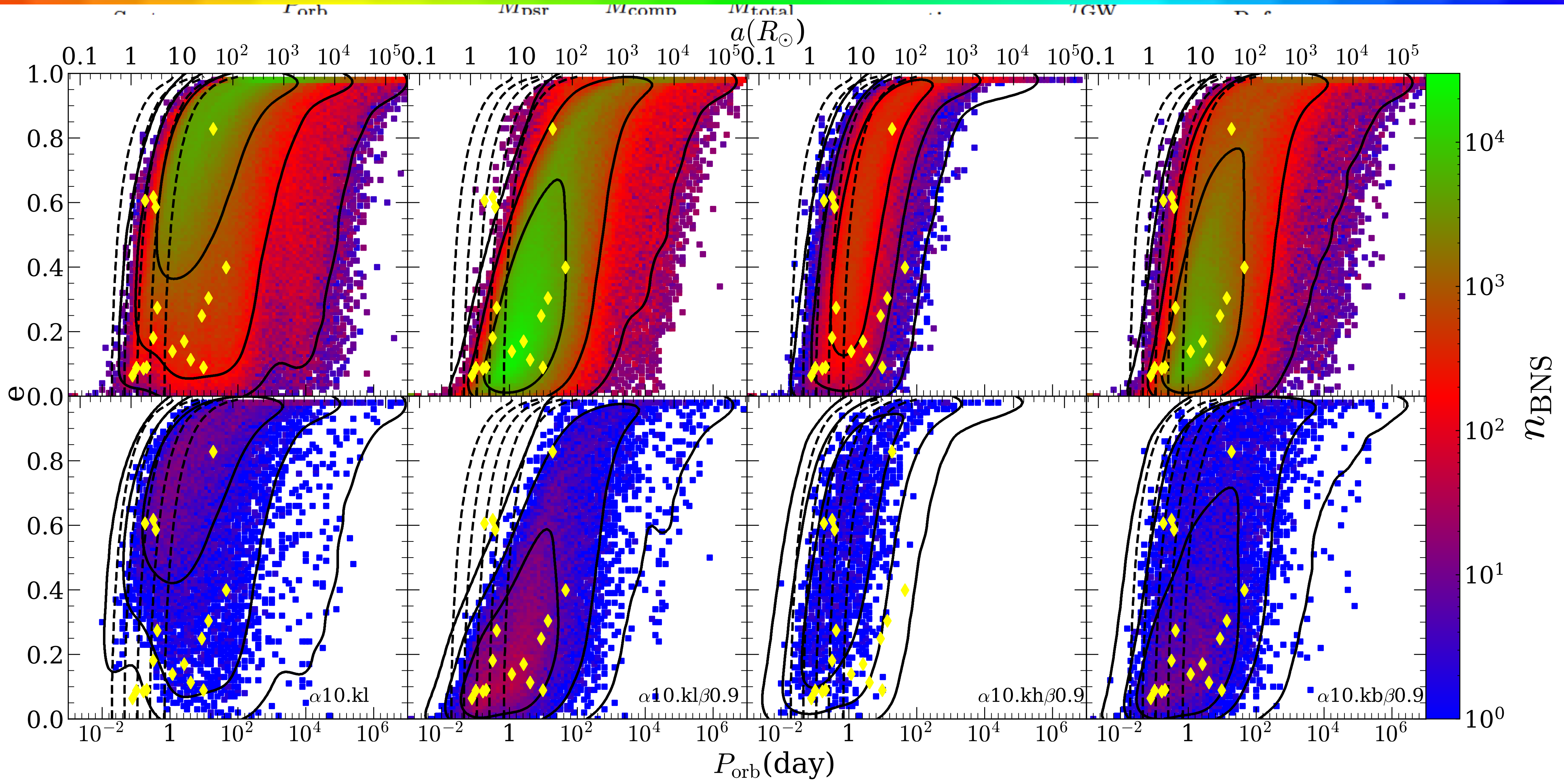

Chu et al. 2022

Galactic BNSs

Model name	log K_i for survived pulsar BNSs				log K_i for all survived BNSs			
		$\beta = 0.6$	$\beta = 0.8$	$\beta = 0.9$		$\beta = 0.6$	$\beta = 0.8$	$\beta = 0.9$
α0.1kl	−77.59	−72.99	−46.91	[illegible]	[illegible]	[illegible]	[illegible]	[illegible]
α0.1kh	−77.83	−82.53	−56.23	[illegible]	[illegible]	[illegible]	[illegible]	[illegible]
α0.1kb	−63.13	−50.46	−25.32	[illegible]	[illegible]	[illegible]	[illegible]	[illegible]
α1.0kl	−58.73	−29.39	−14.64	[illegible]	[illegible]	[illegible]	[illegible]	[illegible]
α1.0kh	−58.72	−54.09	−75.89	[illegible]	[illegible]	[illegible]	[illegible]	[illegible]
α1.0kb	−23.48	−11.59	0.17	[illegible]	[illegible]	[illegible]	[illegible]	[illegible]
α10.kl	−23.70	−22.29	−0.90	[illegible]	[illegible]	[illegible]	[illegible]	[illegible]
α10.kh	−21.36	−11.31	−4.94	−7.47	−27.84	−40.31	−27.21	−32.41
α10.kb	0	−0.50	8.11	9.74	−20.20	−22.56	−24.33	−8.60
γ1.1kl	−57.91	−58.79	−51.15	−50.82	−57.99	−52.72	−51.08	−50.37
γ1.1kh	−47.54	−58.61	−47.54	−51.62	−30.48	−35.38	−17.60	−33.57
γ1.1kb	−57.39	−53.55	−50.16	−50.06	−47.35	−47.03	−39.38	−44.16
γ1.3kl	−25.96	−25.41	−13.42	−11.20	−35.51	−35.44	−25.53	−27.19
γ1.3kh	−3.86	−3.15	−4.69	−6.84	−21.35	−10.49	−11.55	−27.63
γ1.3kb	−7.68	−8.81	4.71	6.65	−19.49	−23.50	−20.16	−15.18
γ1.5kl	−25.55	−22.61	−0.89	−7.66	−32.65	−20.14	−26.57	−32.14
γ1.5kh	−36.29	−36.81	−39.94	−17.69	−33.11	−38.38	−27.90	−33.18
γ1.5kb	−20.80	−4.66	6.57	8.80	−36.85	−17.09	−19.65	−25.29
γ1.7kl	−25.78	−33.98	−15.18	−13.21	−29.96	−29.27	−21.57	−31.63
γ1.7kh	−22.83	−3.25	−17.22	−4.03	−28.93	−11.74	−40.35	−32.57
γ1.7kb	−6.46	−1.66	3.53	5.65	−19.11	−17.63	−20.62	−20.48

$$\log L_i = \sum_{j=1}^{N_{\rm BNS}} \log p(\log P_{{\rm orb},j}, e_j)|_{{\rm M}_i}$$

$$= \sum_{j=1}^{N_{\rm obs}} \sum_{l=1}^{N_P} \sum_{k=1}^{N_e} N(\log P_{{\rm orb},j}, e_j | \log P_l, e_k, \sigma^2_{\log P_l}, \sigma^2_{e_k})\,|_{{\rm M}_i}$$

Chu et al. 2022

Merger rate density and its cosmic evolution

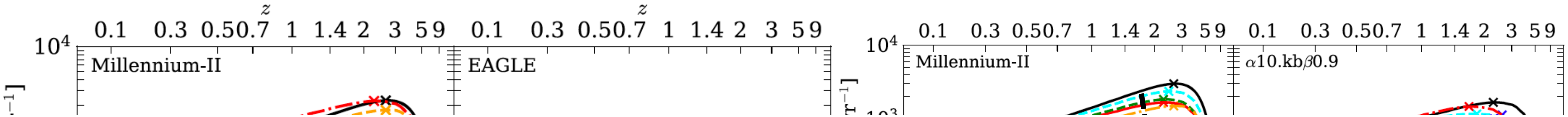

Model name	$R_{\rm Mil,0}$	Millennium-II ζ	$z_\star$	ξ	$R_{\rm EAG,0}$	EAGLE ζ	$z_\star$	ξ	$R_{\rm Ill,0}$	Illustris-TNG ζ	$z_\star$	ξ	$R_{\rm MD,0}$	Madau & Dickinson (2014) ζ	$z_\star$	ξ	$R_{\rm MW}$ [Myr^{-1}]
SFR	–	2.22	3.22	6.25	–	2.78	1.79	4.47	–	1.94	2.87	5.24	–	2.7	1.9	5.6	–
α1.0kbβ0.9	237	1.95	4.49	6.39	177	2.59	2.72	3.96	311	1.69	4.23	5.05	491	2.51	3.05	4.94	44.4
α10.khβ0.9	135	1.84	4.30	6.17	99.8	2.31	2.80	3.90	167	1.56	4.14	5.08	272	2.32	3.01	5.24	25.2
α10.kbβ0.9	421	1.58	4.28	5.98	316	2.03	2.75	3.72	499	1.34	4.08	4.93	784	1.98	3.06	5.10	80.5
γ1.3klβ0.9	447	1.07	3.46	5.21	332	1.33	2.45	3.23	480	0.85	3.27	4.03	784	1.57	2.74	4.33	86.2
γ1.3kbβ0.9	261	1.28	3.99	5.52	194	1.58	2.77	3.44	291	1.04	3.87	4.52	477	1.76	2.90	4.67	50.1
γ1.5kbβ0.9	199	1.66	4.23	6.11	137	2.08	2.98	4.18	228	1.43	4.15	5.44	429	1.98	2.79	4.75	35.5
γ1.7khβ0.9	123	1.74	4.45	6.18	81.3	1.91	3.51	3.82	138	1.45	4.45	5.17	229	2.35	2.95	5.42	21.3
γ1.7kbβ0.9	369	1.33	4.90	6.44	226	1.30	4.81	4.14	368	1.08	5.13	5.57	683	2.10	2.90	5.18	62.9

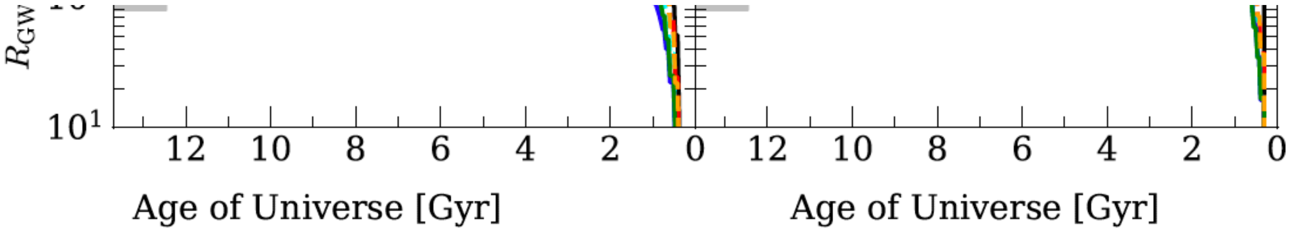

ζ=1.00 γ1.3klβ0.9

$$R_{\rm GW} = N_{\rm mrg}\left(\frac{l_{\rm box}}{\rm Gpc}\right)^{-3}\left(\frac{\Delta t}{\rm yr}\right)^{-1}\,{\rm Gpc^{-3}\,yr^{-1}}.$$

The predicted local merger rate is consistent with observations.

Chu et al. 2022

BNS merger rate

Source	Rate [$\mathrm{Gpc^{-3}\ yr^{-1}}$]	Reference
Models:		
Isolated binary population synthesis, StarTrack	[30, 1700]	O'Shaughnessy et al. (2010)
Isolated binary population synthesis, Scenario Machine	[1050, 3860]	Lipunov and Pruzhinskaya (2014)
Isolated binary population synthesis, Brussels code	[$\lesssim$ 1.3, 1800]	Mennekens and Vanbeveren (2014)
Isolated binary population synthesis, StarTrack	[30, 540]	de Mink and Belczynski (2015)
Isolated binary population synthesis, StarTrack	[52, 162]	Dominik et al. (2015)
Isolated binary population synthesis, BSE	[240, 1800]	Ablimit and Maeda (2018)
Isolated binary population synthesis, StarTrack	[8, 50]	Belczynski et al. (2018a)
Isolated binary population synthesis, StarTrack	[1.5, 631]	Chruslinska et al. (2018)
Isolated binary population synthesis, MOBSE	[10, 510]	Giacobbo and Mapelli (2018)
Isolated binary population synthesis, StarTrack	[24, 68]	Klencki et al. (2018)
Isolated binary population synthesis, COMBINE	[2.7, 159]	Kruckow et al. (2018)
Isolated binary population synthesis, MOBSE	[19, 591]	Mapelli and Giacobbo (2018)
Isolated binary population synthesis, COMPAS	[61.5, 362]	Vigna-Gómez et al. (2018)
Isolated binary population synthesis, MOBSE	238	Artale et al. (2019)
Isolated binary population synthesis, MOBSE	[12, 400]	Baibhav et al. (2019)
Isolated binary population synthesis, SEVN	70	Boco et al. (2019)
Isolated binary population synthesis, StarTrack	[48, 885]	Chruslinska et al. (2019)
Isolated binary population synthesis, BPASS	[339, 2178]	Eldridge et al. (2019)
Isolated binary population synthesis, COMPAS	[20, 245]	Neijssel et al. (2019)
Isolated binary population synthesis, StarTrack	[49.3, 524]	Belczynski et al. (2020)
Isolated binary population synthesis, MOBSE	[20, 640]	Giacobbo and Mapelli (2020)
Isolated binary population synthesis, MOBSE	283^{+97}_{-75}	Santoliquido et al. (2020)
Isolated binary population synthesis, BPASS	[394, 3190]	Tang et al. (2020)
Isolated binary population synthesis, COSMIC	[600, 8900]	Zevin et al. (2020)
Isolated binary population synthesis, BSE,	[0.4, 1404]	Chu et al. (2021)
Isolated binary population synthesis, BPASS	[43, 745]	Ghodla et al. (2021)
Isolated binary population synthesis, StarTrack	[148, 322]	Olejak et al. (2021)
Isolated binary population synthesis, MOBSE	[4.3, 1036.8]	Santoliquido et al. (2021)
Isolated binary population synthesis, BPASS,	27	Briel et al. (2022b)
Isolated binary population synthesis, COMPAS	[0.32, 330]	Broekgaarden et al. (2021, 2022)
Isolated binary population synthesis, StarTrack	[116, 155]	Olejak et al. (2022)
Hierarchical triples, SecularMultiple	[164, 3793]	Hamers and Thompson (2019)
Hierarchical quadruples, MSE	[0.8, 30.2]	Vynatheya and Hamers (2021)
Globular cluster dynamics	30	Lee et al. (2010)
Globular cluster dynamics	[0.32, 3.2]	Bae et al. (2014)
Globular cluster dynamics	121	Samsing et al. (2014)
Globular cluster dynamics, MOCCA	[0.02, 0.5]	Belczynski et al. (2018a)
Globular cluster dynamics, CMC	[0.009, $\lesssim$ 25.5]	Ye et al. (2020)
Nuclear star cluster dynamics with SMBH	[0.004, 1.4]	Antonini and Perets (2012)
Nuclear star cluster dynamics, with SMBH	$\lesssim$ 0.02	Petrovich and Antonini (2017)
Nuclear star cluster dynamics	[0.007, 0.1]	Belczynski et al. (2018a)
Nuclear star cluster dynamics, with SMBH	[0.06, 0.1]	Fragione et al. (2019)
Nuclear star cluster dynamics, with SMBH	$\lesssim$ 400	McKernan et al. (2020)
Nuclear star cluster dynamics, with SMBH	$\gtrsim$ [0.15, 0.3]	Wang et al. (2021)
Young star clusters	[0.03, 0.15]	Ziosi et al. (2014)
Young/Open star clusters, Nbody7	[0.01 – 0.1]	Fragione and Banerjee (2020)
Young star clusters, MOBSE	151^{+59}_{-38}	Santoliquido et al. (2020)

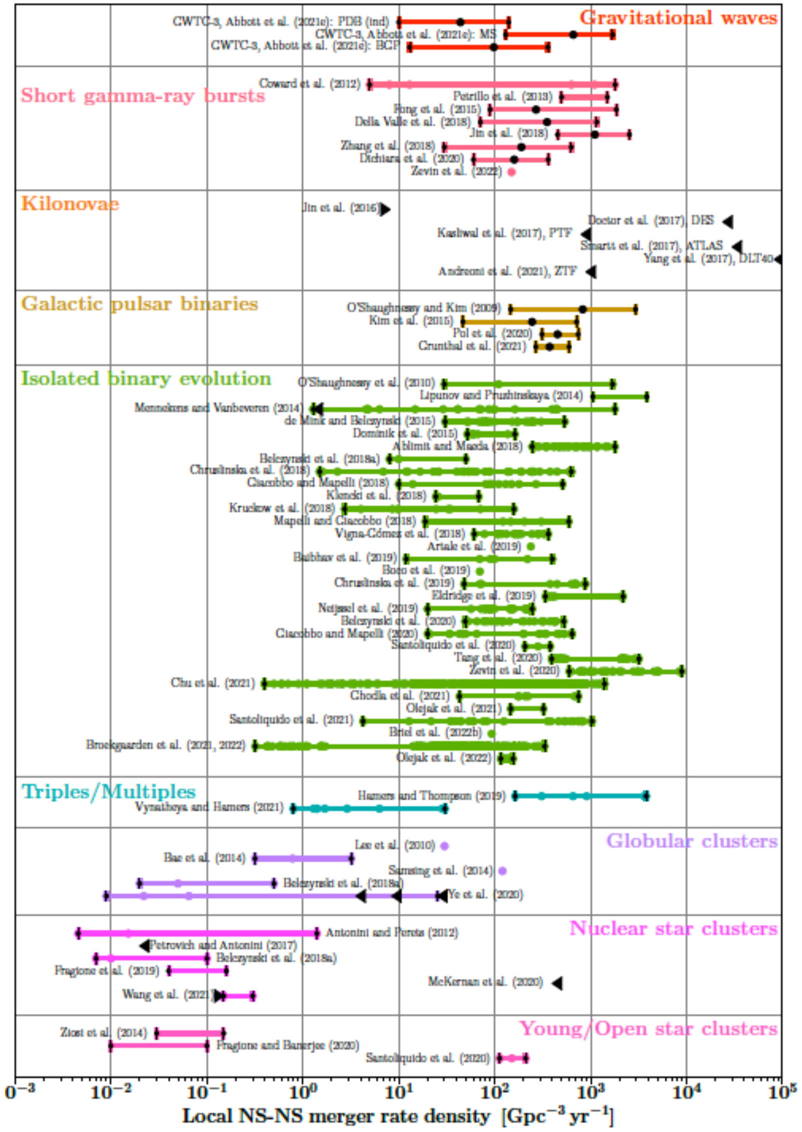

Mandel & Broekgaarden 2022, LRR

Multiband Electromagnetic counterparts

Eric 2019

BNS mergers
GW and EM

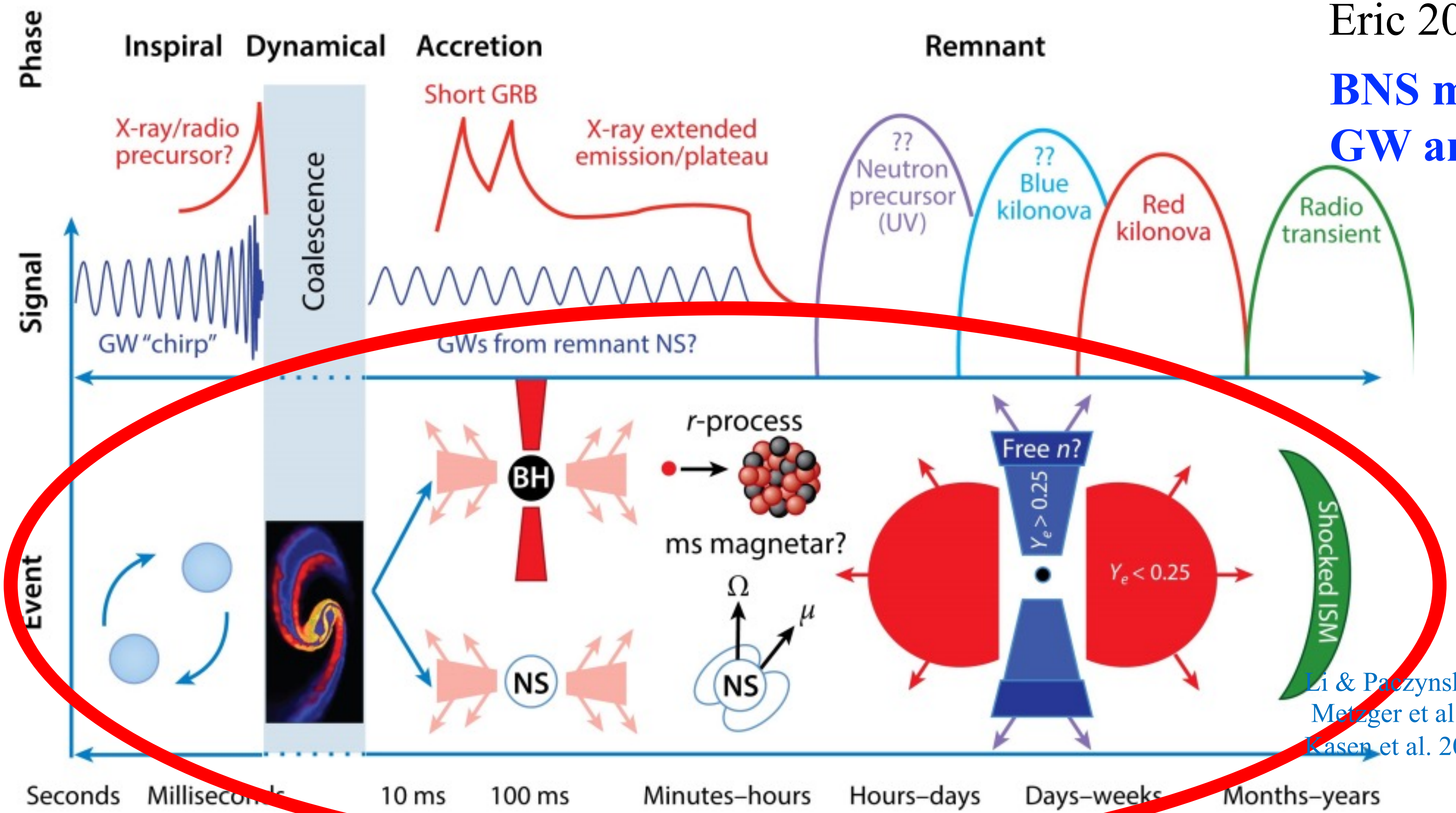

Li & Paczynski, 1998, ApJL
Metzger et al. 2010, MNRAS
Kasen et al. 2017, Nature

Multiband Electromagnetic counterparts

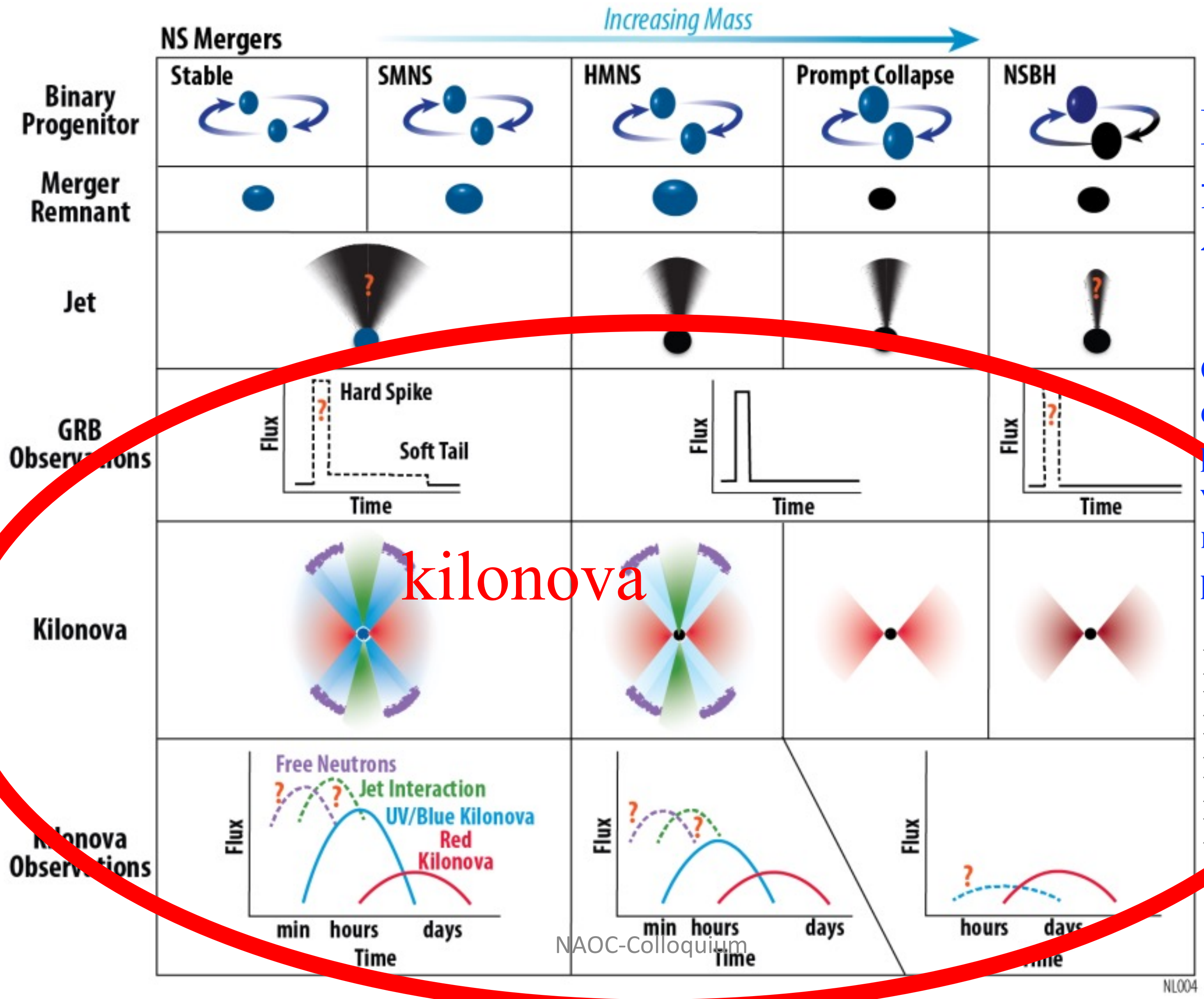

Eric 2019

EM counterparts from different types of mergers

Observational signals are determined by the ejecta properties, including mass, velocity, structure, and microphysics and radiation processes

- **Dynamical ejecta**
- **Remnant disk**
- **Disk wind**
- **Fallback accretion**
- **……**

Kilonovae from BNS mergers

GR numerical simulations

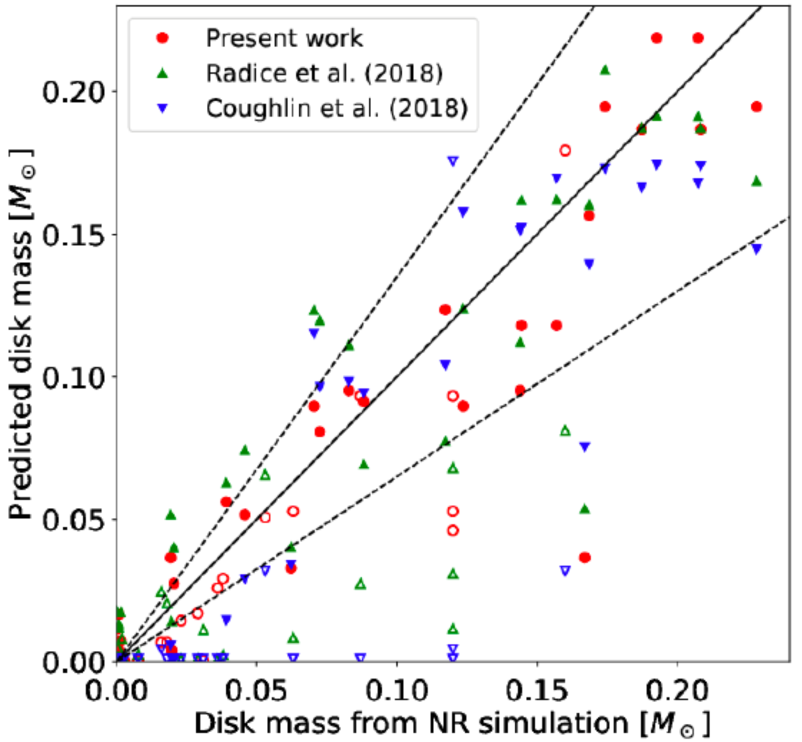

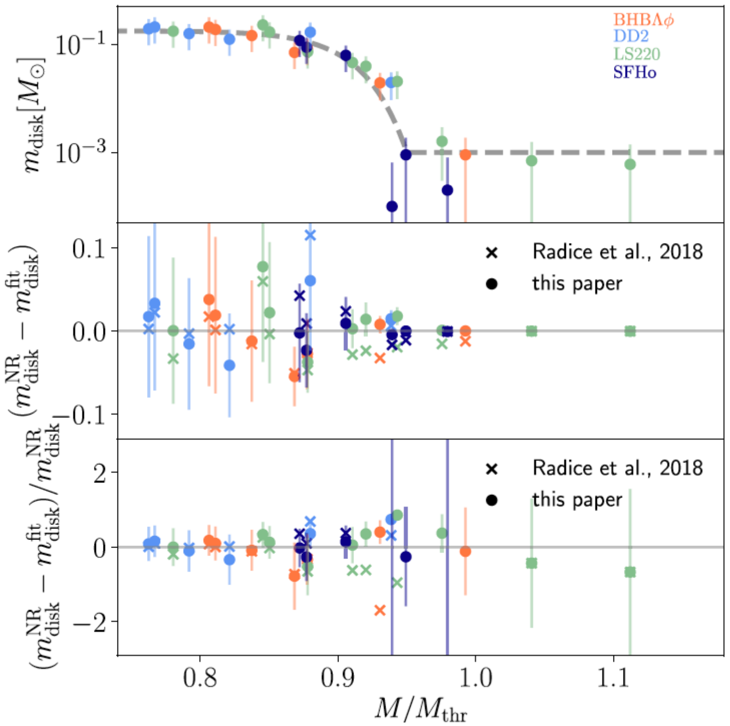

$$\frac{m_{\rm dyn}^{\rm JKF}}{10^{-3}M_\odot} = \left(\frac{a_1}{C_1} + a_2\frac{m_2^{n_1}}{m_1^{n_1}} + a_3 C_1\right) m_1 + (1 \leftrightarrow 2)$$

$$\frac{m_{\rm disk}^{\rm JKF}}{M_\odot} = m_1 \left[\max\left(e_1 C_1 + e_2,\ 5\times 10^{-4}\right)\right]^{n_3}$$

$$\log\left(\frac{m_{\rm dyn}^{\rm COU}}{M_\odot}\right) = \left[b_1 m_1 \frac{(1-C_1)}{C_1} + b_2 m_2 \left(\frac{m_1}{m_2}\right)^{n_2} + \frac{b_3}{2}\right] + (1 \leftrightarrow 2)$$

$$\log\left(\frac{m_{\rm disk}^{\rm COU}}{M_\odot}\right) = \max\left[-3, d_1\left(1 + d_2 \tanh\left[\frac{d_3 - m_{\rm tot}/M_{\rm thr}}{d_4}\right]\right)\right]$$

In addition, results for the velocity and opening angle for dynamical ejecta

Kruger & Foucart 2020, PRD

Coughlin et al. 2019, MNRAS

Phenomenological kilonova model

- **Dynamical ejecta** (mass, velocity, structure)
  - ❑ Red component
  - ❑ Blue component
- **Disk wind** (mass, velocity, structure)
  - ❑ Viscous-driven wind
    purple+red components
  - ❑ Neutrino-driven wind
    blue+purple components
- **Fallback accretion** (mass)
  Heating, isotropic radiation
- **Photosphere of the ejecta**
  R-process heating
- **Emergent luminosity**
- **Kilonova light curves**
  MOSFiT

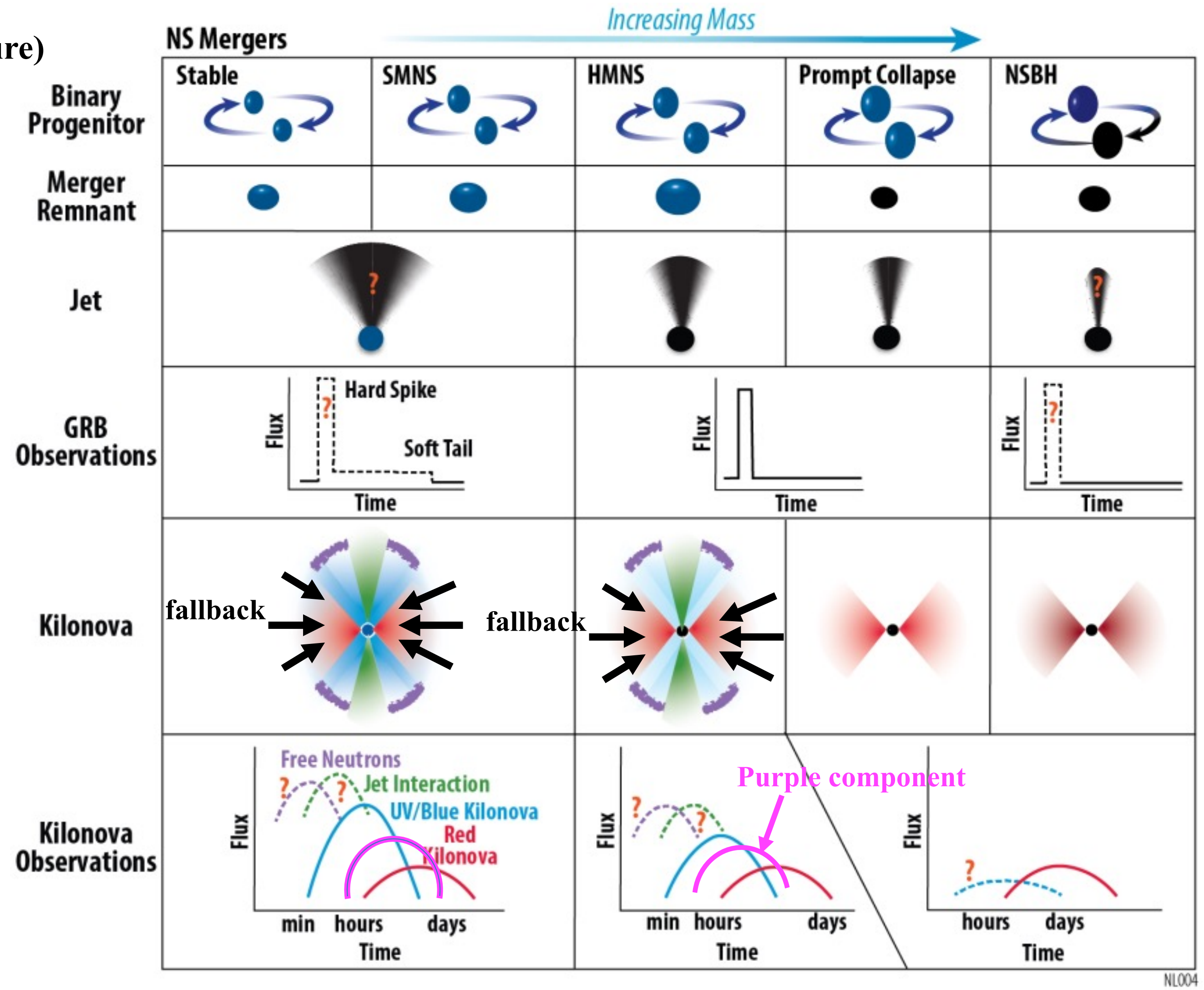

Kilonova models

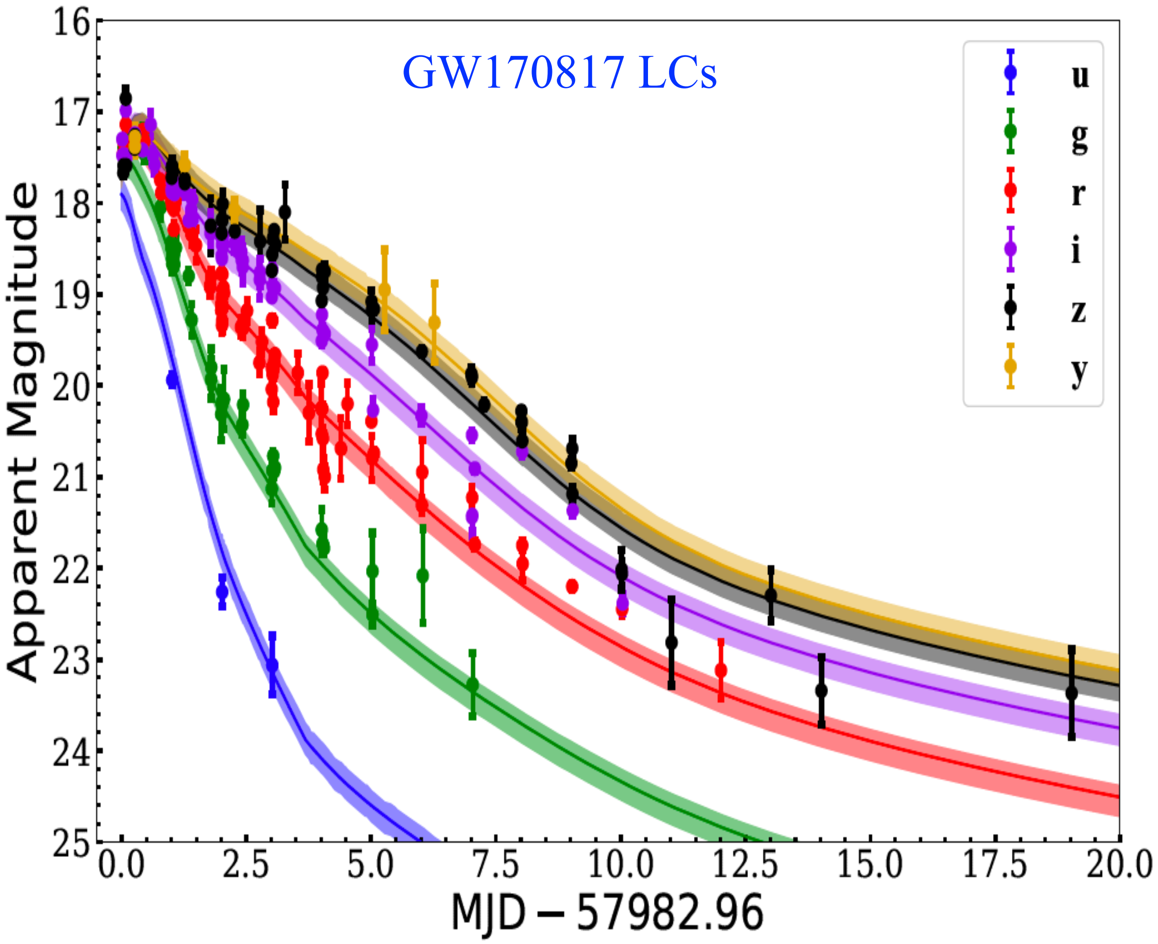

Contributions from different components

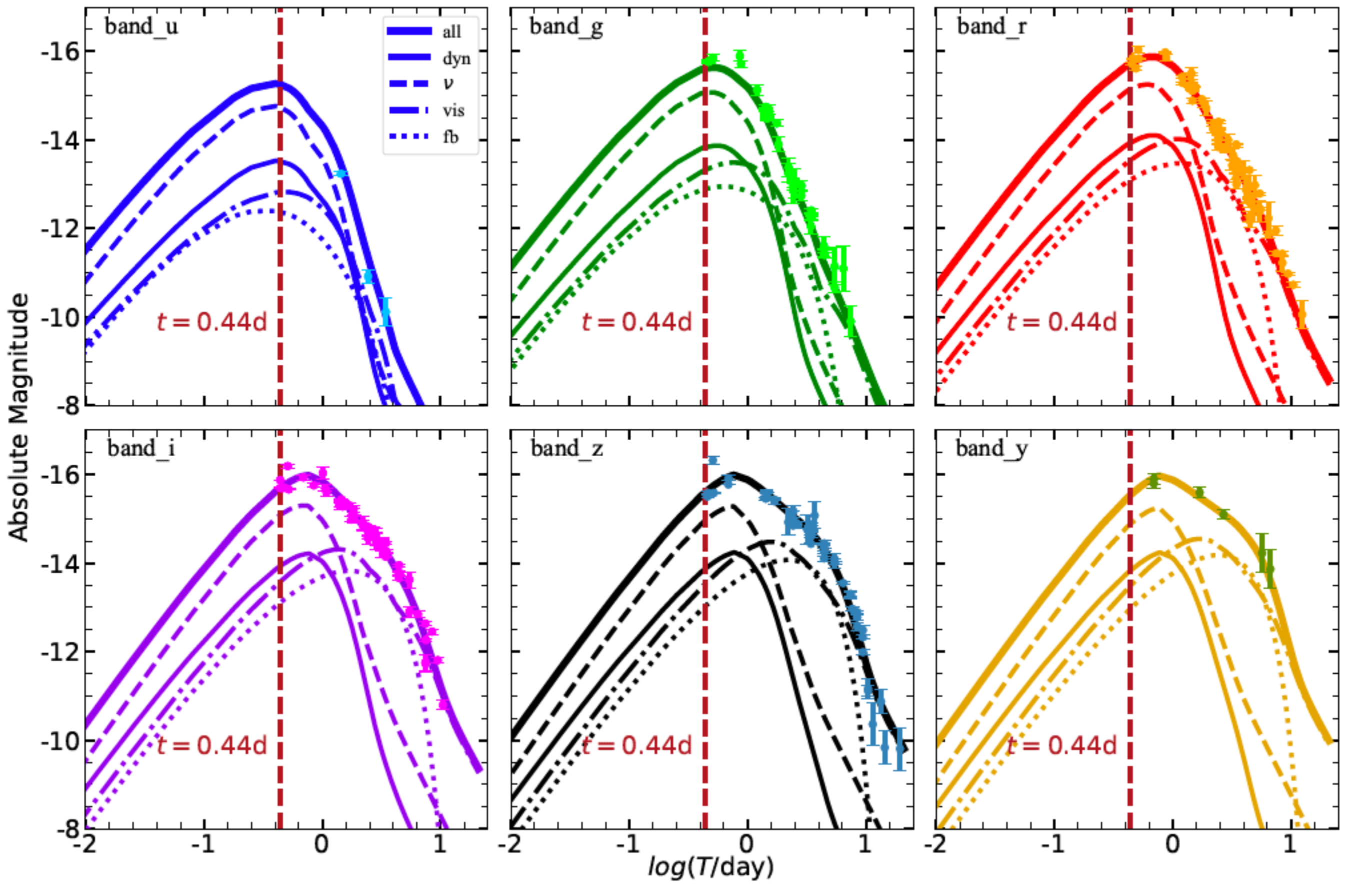

Model fitting to the light curves of GW170817

Zhao et al. 2022, submitted to MNRAS

Kilonova models

$\log\left(\frac{m_{\rm disk}}{M_\odot}\right)$	$\frac{m_{\rm ej}^{\rm d}}{10^{-3}M_\odot}$	$\theta_{\rm db}(^\circ)$	$\frac{v_{\rm dyn}}{\rm c}$	$\frac{t_{\rm n}}{\rm day}$	$\epsilon_{\rm dec}$
$-0.85^{+0.06}_{-0.06}$	$5.9^{+0.6}_{-0.2}$	$31.2^{+1.9}_{-1.4}$	$0.336^{+0.044}_{-0.039}$	$1.00^{+0.30}_{-0.43}$	$2.03^{+1.13}_{-0.66}$
$\epsilon_{\rm n}$	$\log\left(\frac{\epsilon_0}{\rm erg\ s^{-1}}\right)$	$\log\left(\frac{\dot{M}_{\rm fb}}{M_\odot{\rm s}^{-1}}\right)$	$\frac{m_{\rm ph}^{\rm fb}}{10^{-3}M_\odot}$	ξ_ν	$\xi_{\rm vis}$
$1.81^{+0.84}_{-0.23}$	$18.91^{+0.02}_{-0.03}$	$-2.65^{+0.008}_{-0.008}$	$5.25^{+0.14}_{-0.15}$	$0.023^{+0.005}_{-0.006}$	$0.280^{+0.018}_{-0.020}$
$\theta^{\nu{\rm b}}(^\circ)$	$\theta^{\nu{\rm p}}(^\circ)$	$\theta_{\rm v}(^\circ)$	$\frac{\kappa_{\rm b}}{\rm cm^2g^{-1}}$	$\frac{\kappa_{\rm p}}{\rm cm^2g^{-1}}$	$\frac{\kappa_{\rm r}}{\rm cm^2g^{-1}}$
49^{+13}_{-7}	81^{+5}_{-10}	$22^{+1.00}_{-3.20}$	$1.39^{+0.06}_{-0.12}$	$2.30^{+0.15}_{-0.11}$	$32.0^{+2.89}_{-1.72}$
$\frac{\kappa_{\rm fb}}{\rm cm^2g^{-1}}$	$\frac{T_{\rm f,b}}{\rm K}$	$\frac{T_{\rm f,p}}{\rm K}$	$\frac{T_{\rm f,r}}{\rm K}$	$\frac{T_{\rm f,fb}}{\rm K}$	$\frac{v_{\rm fb}}{\rm c}$
$26.80^{+6.76}_{-5.31}$	6388^{+287}_{-247}	3172^{+62}_{-41}	460^{+138}_{-217}	1051^{+69}_{-79}	$0.134^{+0.008}_{-0.004}$
$\frac{v_{\nu{\rm b}}}{\rm c}$	$\frac{v_{\nu{\rm p}}}{\rm c}$	$\frac{v_{\rm visp}}{\rm c}$	$\frac{v_{\rm visr}}{\rm c}$	σ	
$0.322^{+0.042}_{-0.027}$	$0.166^{+0.037}_{-0.018}$	$0.230^{+0.010}_{-0.007}$	$0.220^{+0.008}_{-0.007}$	$0.16^{+0.006}_{-0.004}$	

The best-fit model parameters

Zhao et al. 2022

Kilonova assoiated with GW190425

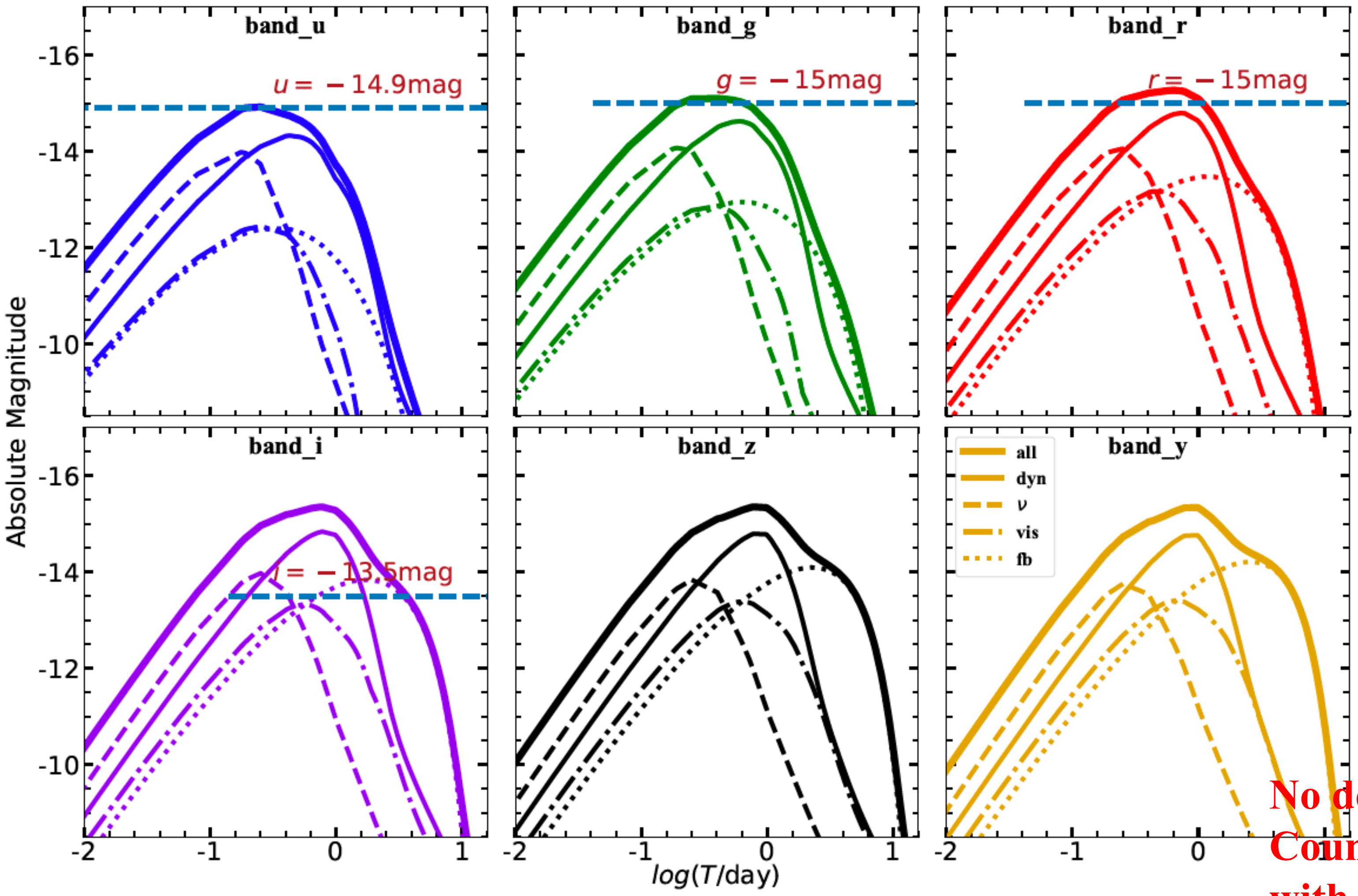

No detection of EM Counterparts is consistent with model predictions

Dark blue dashed lines: the observational upper limits

Zhao et al. 2022

Kilonova peak luminosities

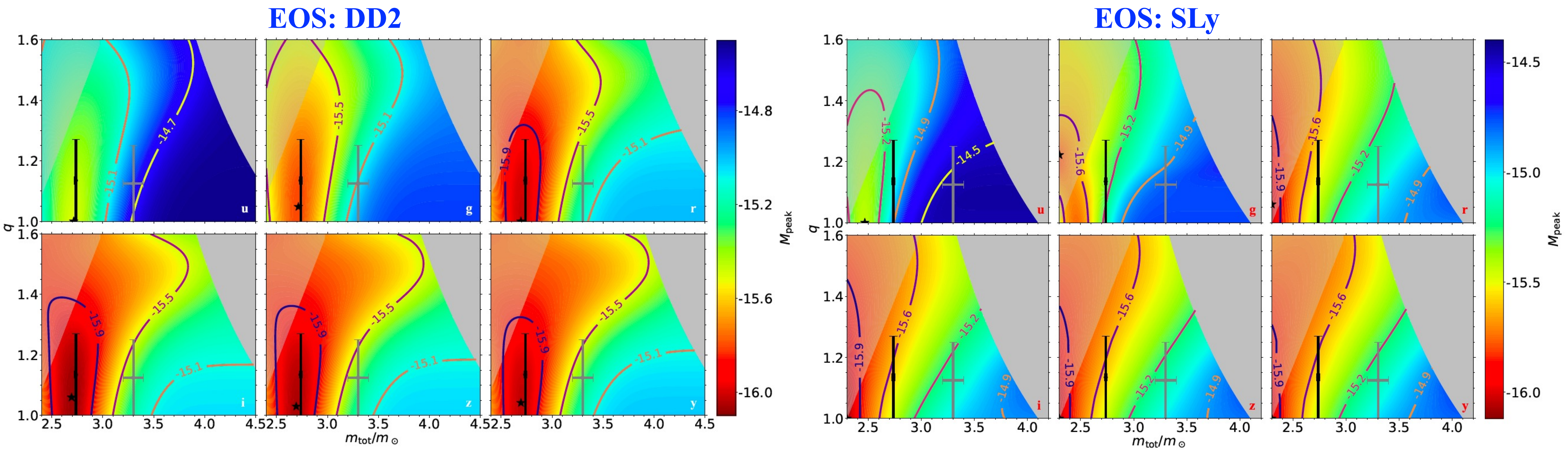

- **BNS mergers with same q under the same EOS**: larger total mass, fainter peak luminosities, and more rapid decay of the light curves after the peak luminosity, because of lighter disk formed in BNS mergers with larger total mass;
- **BNS mergers with same total mass under the same EOS:** the larger the mass ratio when the total mass is large, the brighter the peak luminosities, because of more massive disk formed in mergers with larger mass ratio；
- **BNS mergers with same total mass and mass ratio:** the stiffer the EOS, the brighter the peak luminosities because of more neutrons ejected in the case with a stiff EOS compared with that with a softer EOS.

Zhao et al. 2022

Maximum “detctable” kilonova distances

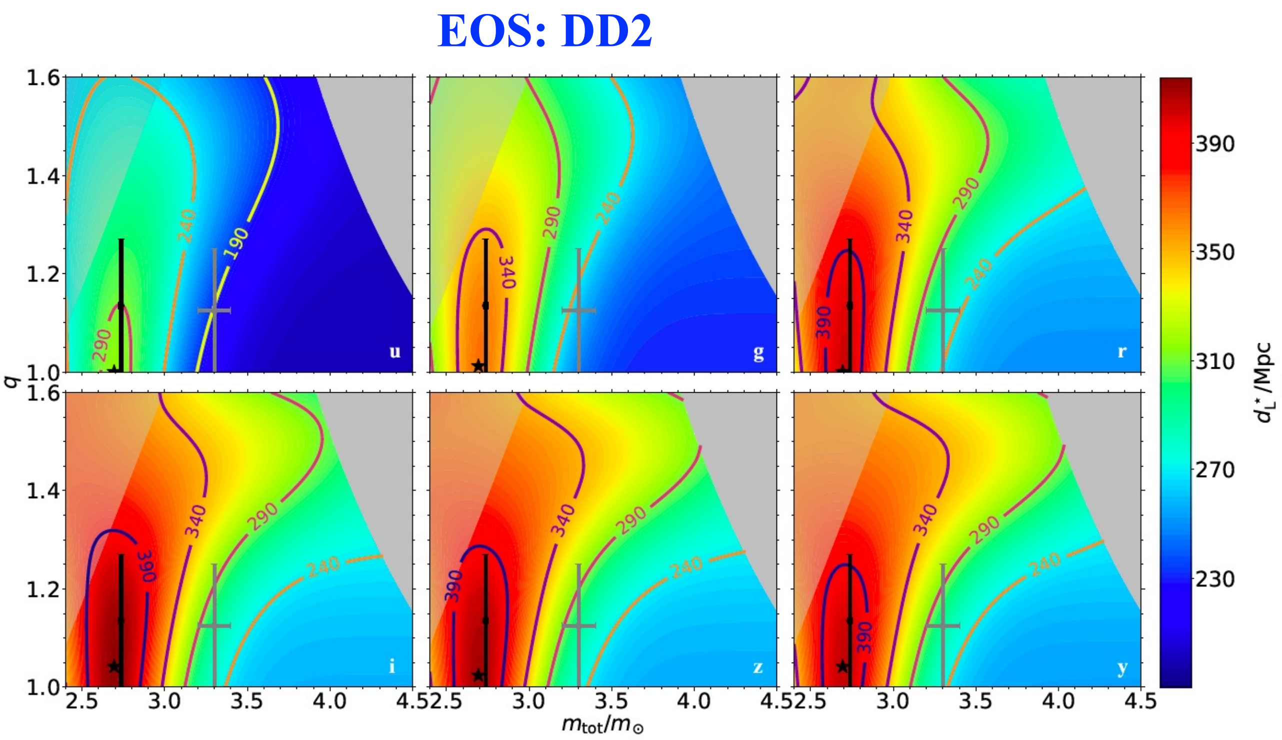

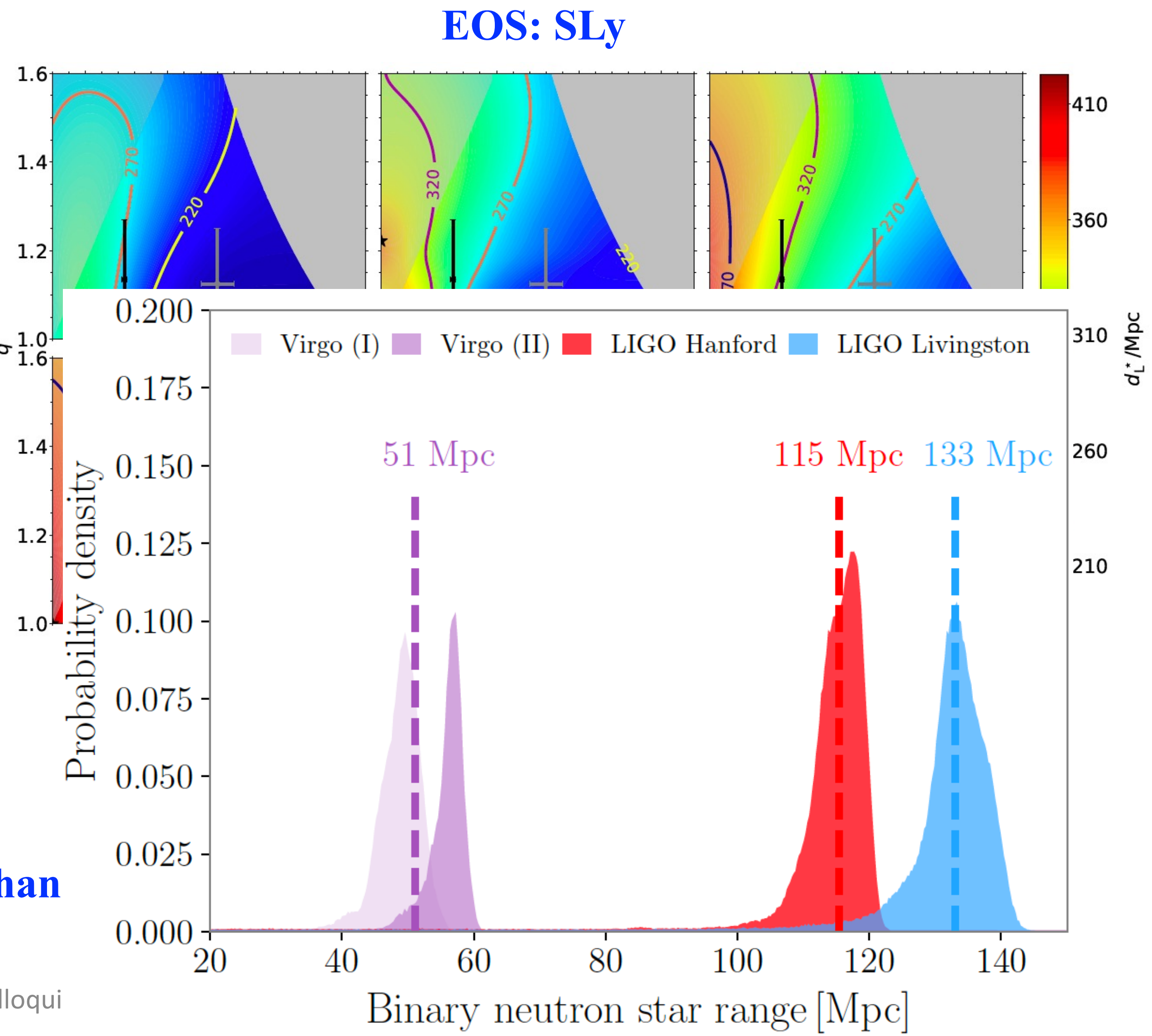

$$d_{\rm L,max} = 10^{0.2(m_{\rm app}-22)} d^*_{\rm L,max}.$$

O4: LIGO, 160-190 Mpc; Virgo, 80-115 Mpc

Required search magnitude limit should not be smaller than ~20/22 at g-band for GW170817/GW190425 like sources

Distribution of BNS total mass and mass ratio

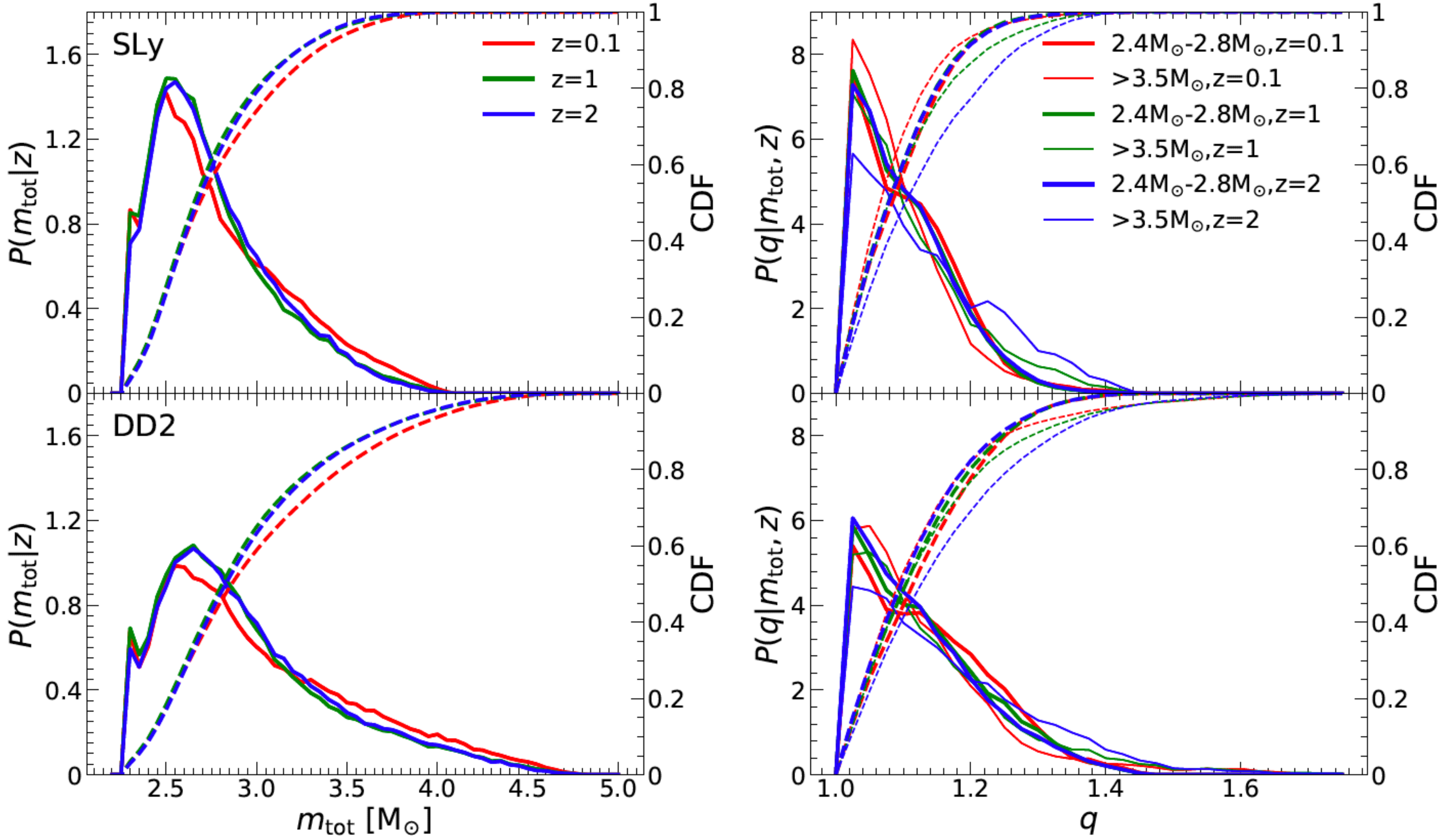

Zhao et al. 2022

Kilonova Luminosity Functions

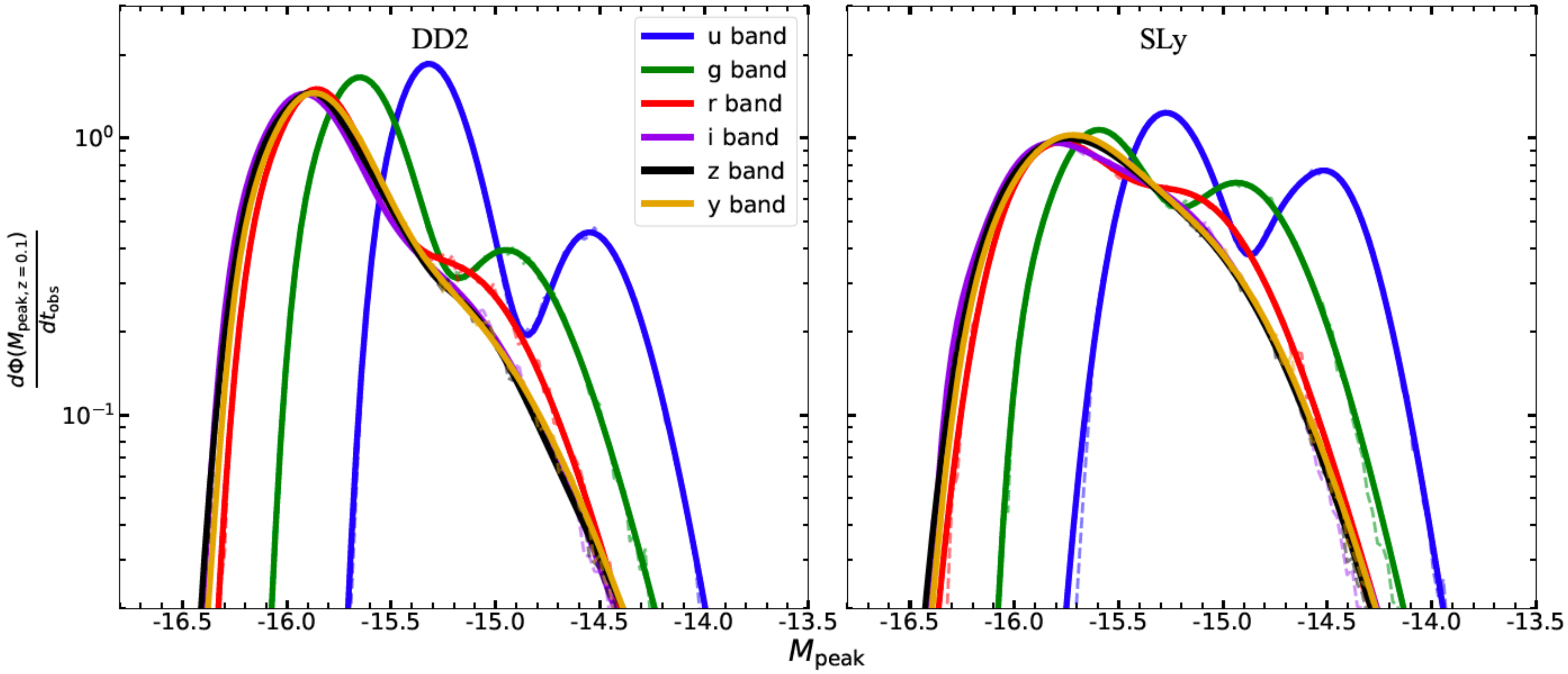

Double peak normalized luminosity function;
EOS dependend but weak redshift evolution;

Zhao et al. 2022

Detection of kilonovae

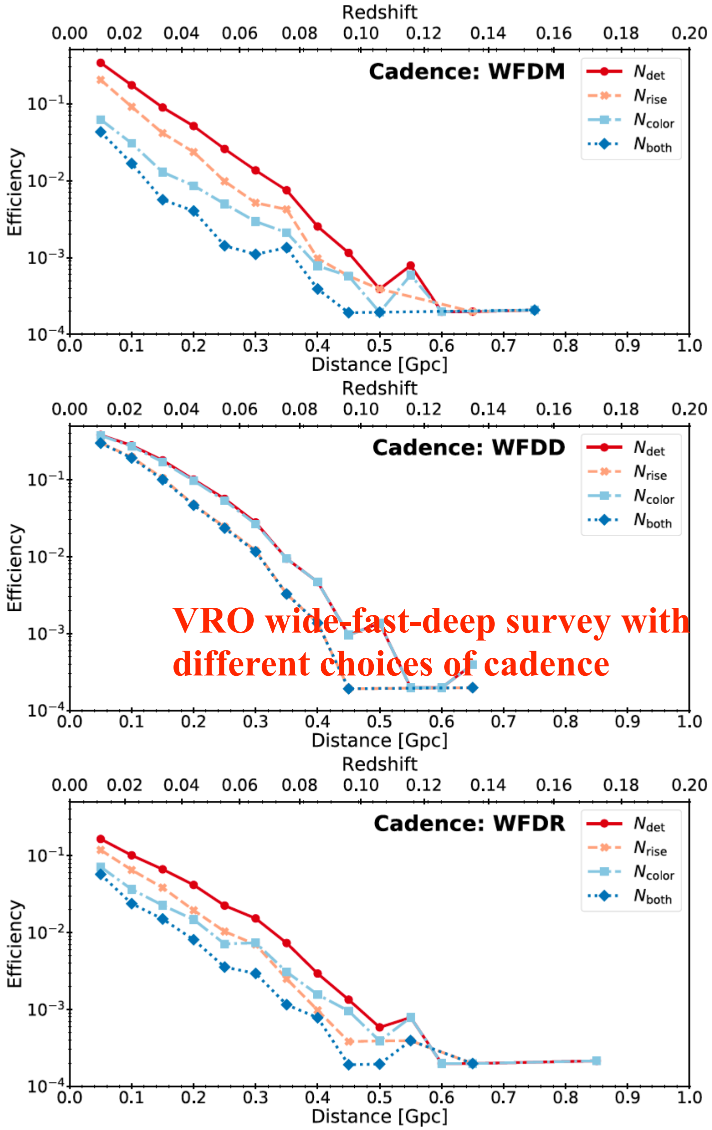

VRO wide-fast-deep survey with different choices of cadence

Cowperthwaite et al. 2019

Summary of WFD Survey Kilonova Detection Efficiencies and Rates

Cadence	$\epsilon_{det}(N_{det})$ $(-(yr^{-1}))$	$\epsilon_{rise}(N_{rise})$ $(-(yr^{-1}))$	$\epsilon_{color}(N_{color})$ $(-(yr^{-1}))$	$\epsilon_{both}(N_{both})$ $(-(yr^{-1}))$	$\epsilon_{<200\ Mpc}(N_{<200\ Mpc})$ $(-(yr^{-1}))$	$\epsilon_{<450\ Mpc}(N_{<450\ Mpc})$ $(-(yr^{-1}))$
WFDM	1.6% (3.7)	0.8% (1.7)	0.3% (0.8)	0.2% (0.4)	14% (1.9)	6.8% (3.5)
WFDD	2.5% (6.6)	1.6% (3.4)	2.4% (6.4)	1.6% (3.3)	22% (3.4)	11% (6.5)
WFDR	1.0% (3.0)	0.6% (1.5)	0.4% (1.3)	0.3% (0.6)	8.5% (1.3)	4.3% (2.9)

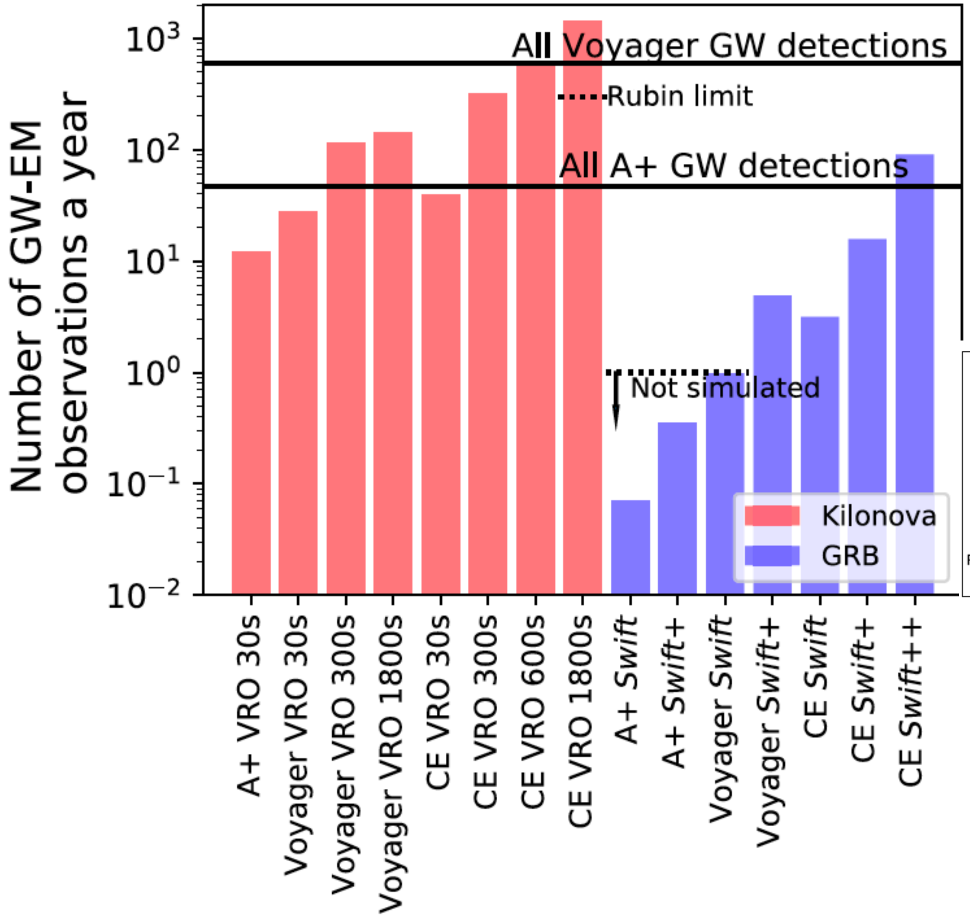

VRO Target of opportunity observations with different choices of exposure time

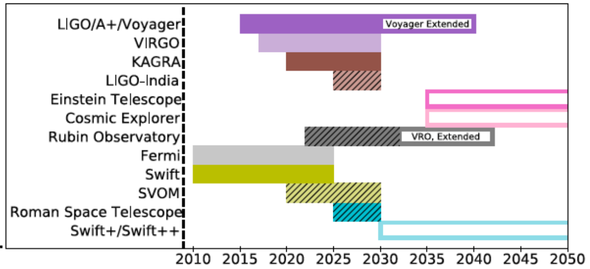

Chen et al. 2021, ApJ

Detection of kilonovae

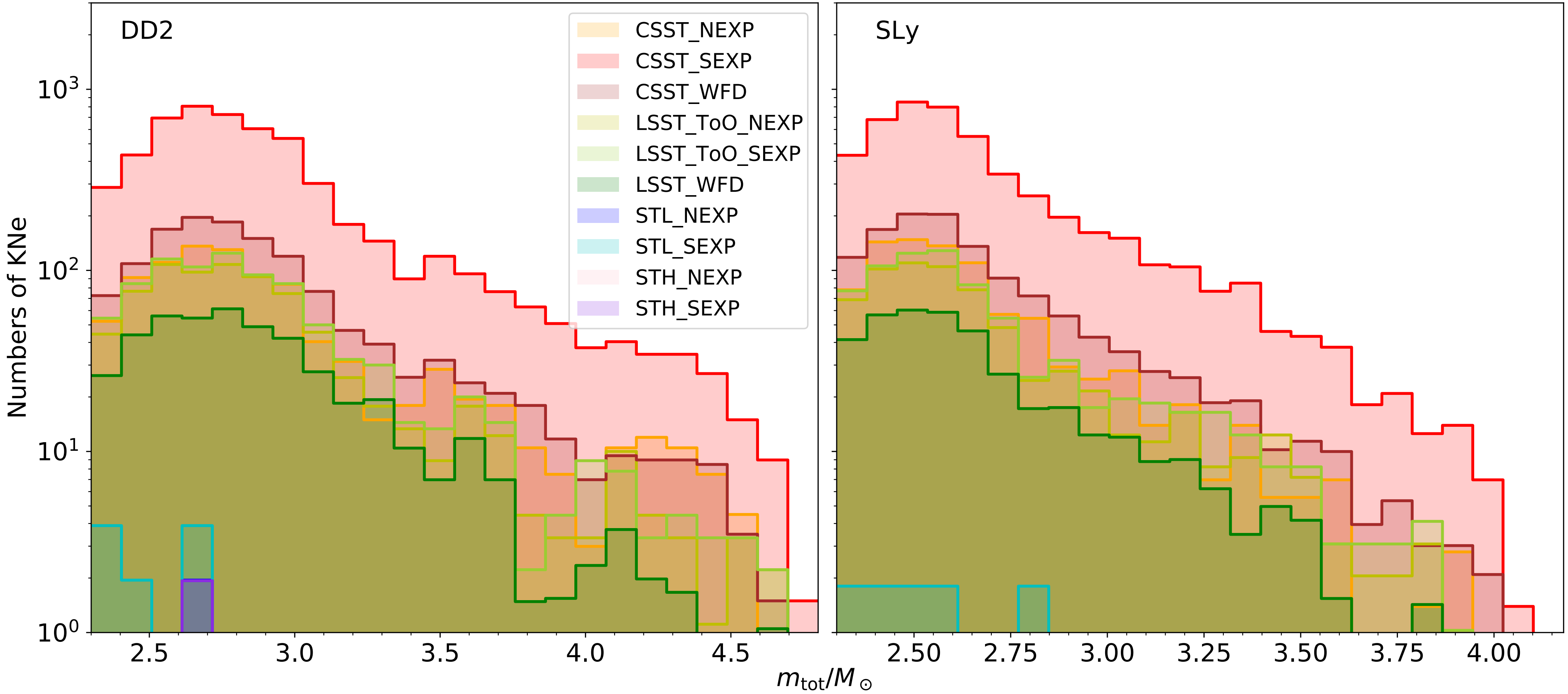

Hundreds to thousands kilonovae are expected to be detected in near future, some may have extreme parameters.

Zhao et al. 2022, in preparation

Detection of lensed kilonovae

Detector	ϱ_0	doub	quad	total	quad*	total*	detectable
LIGO A+	5	6.38×10^{-4}	1.15×10^{-3}	1.79×10^{-3}	1.73×10^{-4}	8.11×10^{-4}	2.18×10^{2}
LIGO A+	8	4.97×10^{-5}	1.81×10^{-4}	2.31×10^{-4}	1.02×10^{-5}	5.99×10^{-5}	5.37×10^{1}
LIGO A+	10	1.25×10^{-5}	3.98×10^{-5}	5.23×10^{-5}	1.98×10^{-6}	1.44×10^{-5}	2.76×10^{1}
LIGO Voyager	5	9.92×10^{-2}	1.08×10^{-1}	2.07×10^{-1}	2.34×10^{-2}	1.23×10^{-1}	3.22×10^{3}
LIGO Voyager	8	7.85×10^{-3}	1.10×10^{-2}	1.88×10^{-2}	2.00×10^{-3}	9.84×10^{-3}	7.87×10^{2}
LIGO Voyager	10	2.15×10^{-3}	3.64×10^{-3}	5.79×10^{-3}	4.81×10^{-4}	2.63×10^{-3}	4.04×10^{2}
ET	5	1.81×10^{1}	5.46×10^{0}	2.36×10^{1}	2.60×10^{0}	2.07×10^{1}	1.10×10^{5}
ET	8	3.45×10^{0}	1.87×10^{0}	5.32×10^{0}	6.47×10^{-1}	4.10×10^{0}	2.89×10^{4}
ET	10	1.30×10^{0}	9.03×10^{-1}	2.20×10^{0}	2.67×10^{-1}	1.57×10^{0}	1.48×10^{4}
CE	5	1.26×10^{2}	1.32×10^{1}	1.39×10^{2}	1.02×10^{1}	1.36×10^{2}	5.21×10^{5}
CE	8	5.74×10^{1}	9.85×10^{0}	6.73×10^{1}	6.30×10^{0}	6.37×10^{1}	2.97×10^{5}
CE	10	3.47×10^{1}	7.80×10^{0}	4.25×10^{1}	4.25×10^{0}	3.90×10^{1}	1.95×10^{5}
GLOC	5	1.86×10^{2}	1.47×10^{1}	2.01×10^{2}	1.26×10^{1}	1.99×10^{2}	6.46×10^{5}
GLOC	8	1.05×10^{2}	1.24×10^{1}	1.17×10^{2}	9.23×10^{0}	1.14×10^{2}	4.65×10^{5}
GLOC	10	7.21×10^{1}	1.08×10^{1}	8.29×10^{1}	7.39×10^{0}	7.95×10^{1}	3.57×10^{5}

Upto about one hundred lensed BNS mergers per year are expected to be detected by future GW detectors

Ma et al. 2022, MNRAS

Detection of lensed kilonovae

Euclid/H
Rubin/z
CSST/z
RST/H158
JWST/150W

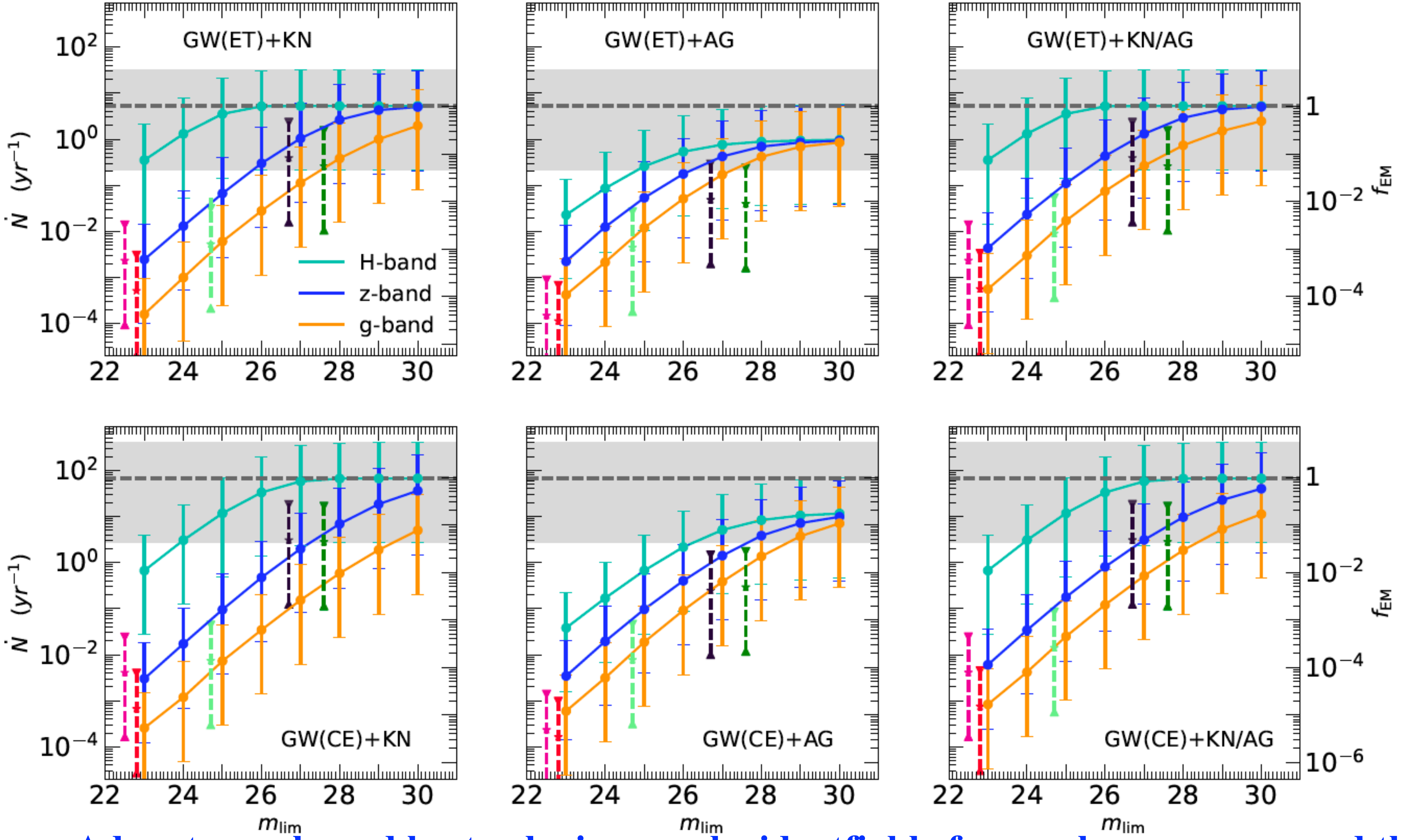

Advantages: lensed host galaxies may be identfiable from galaxy surveys, and thus the lensed kilonovae can be searched by directly pointing to the hosts

Ma et al. 2022

Detection of lensed kilonovae

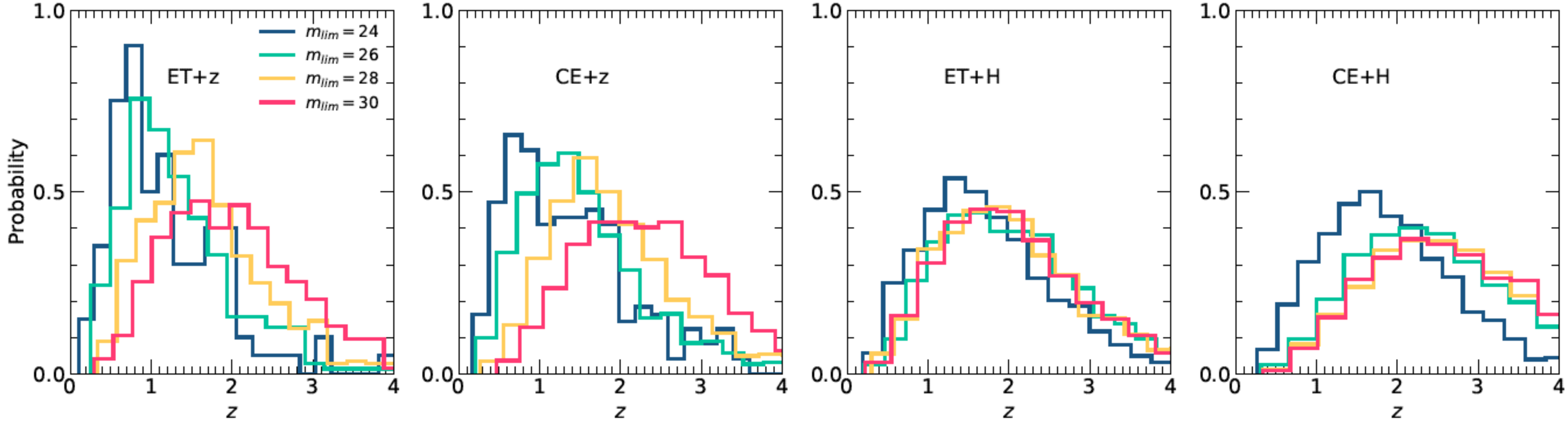

Redshifts of detectable lensed kilonovae peak at ~1-2
Importance for cosmological applications

Ma et al. 2022

Host galaxies of BNS mergers

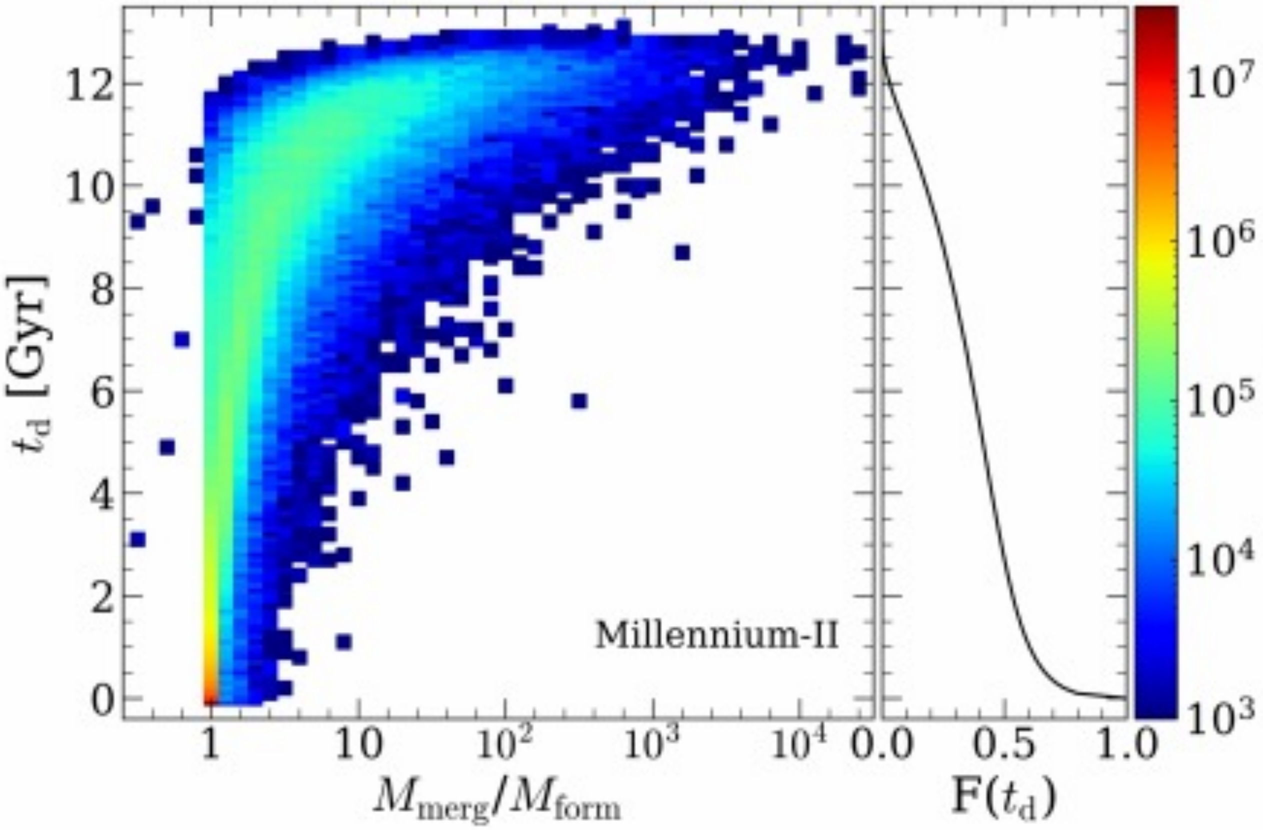

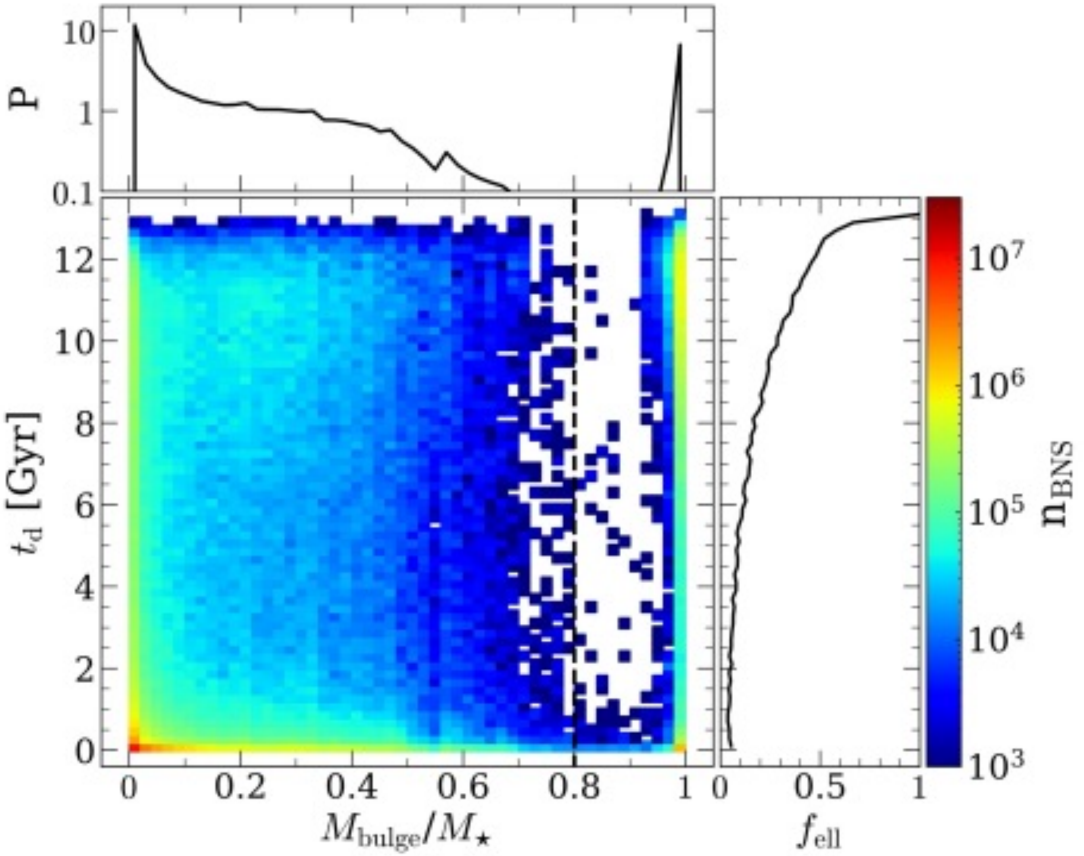

- Galactic BNSs
- BNS merger rate

α10.kbβ0.9

Host galaxy properties versus time-delay of the BNS merger

Host galaxies of BNS mergers: GW170817

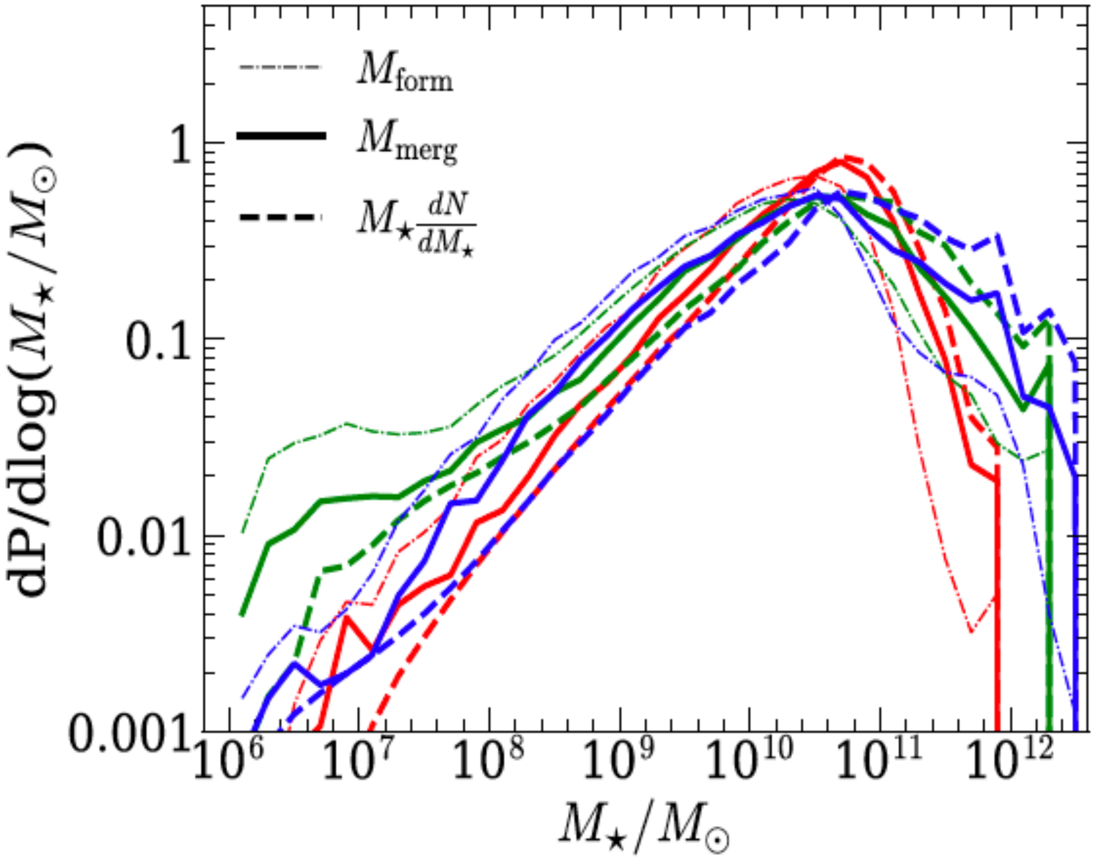

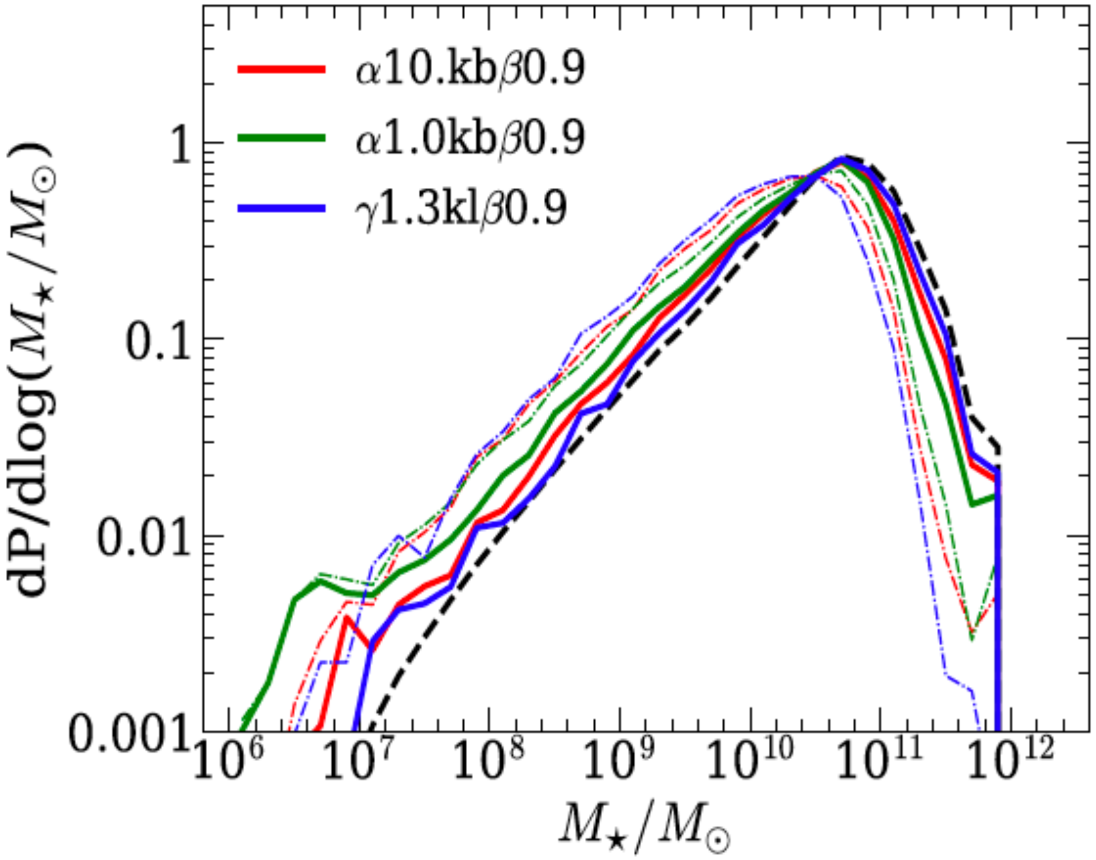

NGC 4993: ~3×10^{10} $M_\odot$-1.2×10^{11} $M_\odot$, elliptical probability: 15.6%/18.8% (red)
Peaks for BNS mergers at merging time:
5.0×10^{10} $M_\odot$, 3.2×10^{10} $M_\odot$ and 3.2×10^{10} $M_\odot$ for Millennium-II, EAGLE and Illustris

Host galaxies of BNS mergers

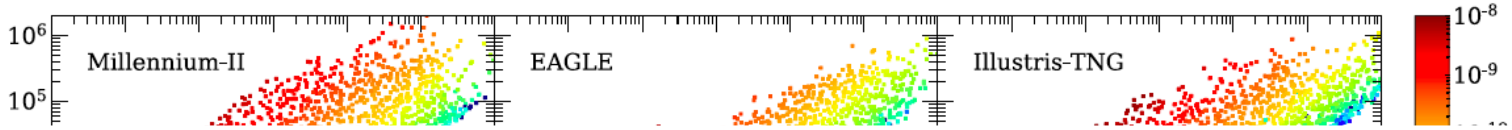

		Millennium-II	EAGLE	Illustris-TNG	
			$z = 0$		
Fit 1D	a_1	0.801(0.757/0.876)	0.691(0.565/0.663)	0.719(0.707/0.891)	0.756(0.697/0.832)
	a_2	−4.28(−4.53/−5.23)	−2.92(−2.83/−3.85)	−3.19(−3.76/−5.31)	−3.69(−3.90/−4.94)
Fit 2D	b_1	0.883(0.856/0.908)	0.716(0.611/0.679)	0.774(0.749/0.902)	0.809(0.759/0.850)
	b_2	0.428(0.361/0.165)	0.377(0.323/0.193)	0.373(0.286/0.075)	0.401(0.323/0.128)
	b_3	0.017(−1.19/−3.57)	1.03(0.318/−1.86)	0.416(−0.987/−4.58)	0.395(−0.786/−3.64)
Fit 3D	c_1	1.050(1.066/1.108)	0.916(0.863/0.876)	0.948(0.922/0.962)	0.900(0.888/0.967)
	c_2	0.410(0.334/0.143)	0.572(0.567/0.383)	0.522(0.434/0.126)	0.439(0.379/0.178)
	c_3	−0.336(−0.445/−0.406)	−0.469(−0.585/−0.459)	−0.436(−0.432/−0.149)	−0.199(−0.287/−0.257)
	c_4	−1.95(−3.73/−5.94)	1.21(0.548/−1.69)	0.205(−1.20/−4.65)	−0.118(−1.51/−4.30)

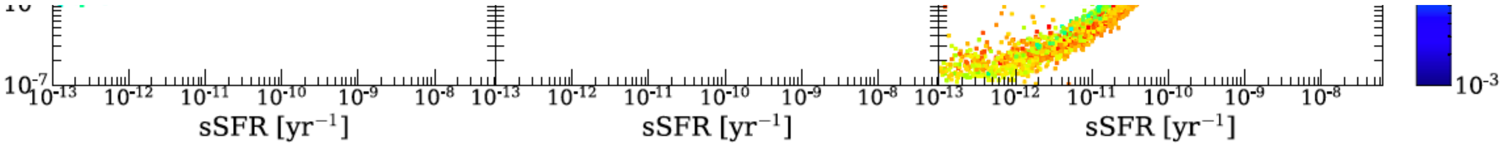

$$\log\left(\frac{n_{\rm GW}}{\rm Gyr}\right) = c_1 \log\left(\frac{M_\star}{M_\odot}\right) + c_2 \log\left(\frac{\rm sSFR}{\rm yr^{-1}}\right) + c_3 \log\left(\frac{Z}{Z_\odot}\right) + c_4$$

Host galaxies of BNS mergers

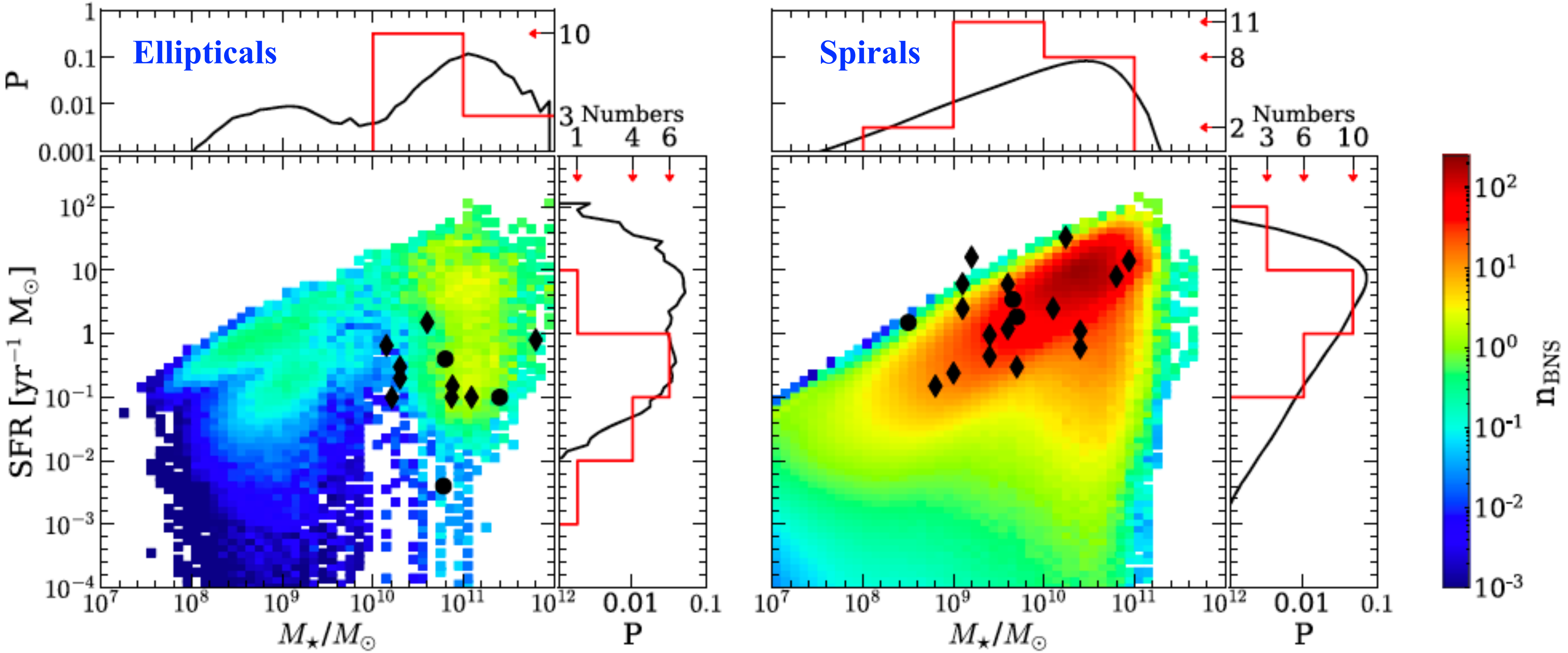

sGRB and kilonova host galaxies						
GRB 130603B	0.3568	Spiral	9.7	–	1.84	Cucchiara et al. (2013)
GRB 150101B	0.1343	Elliptical	10.68-10.92	2-2.5	$\lesssim$0.4	Fong et al. (2016)
GRB 160821B	0.162	Spiral	8.[illegible]	–	$\lesssim$1.5	Troja et al. (2019)
GRB 170817A	0.02	Elliptical	10.48-11.08	$\gtrsim$3	0.004	Im et al. (2017)
GRB 200522A	0.5536	Spiral	9.656	0.531	2.1–4.8	Fong et al. (2021)
GRB 070809	0.473	Elliptical	11.4	3.10	<0.1	Berger (2014), Jin et al. (2020)
	0.219	Spiral	10.3	–	–	Perley et al. (2008), Jin et al. (2020)

The properties of the sGRB host galaxies are consistent with those of kilonovae and BNS mergers.

Prospects

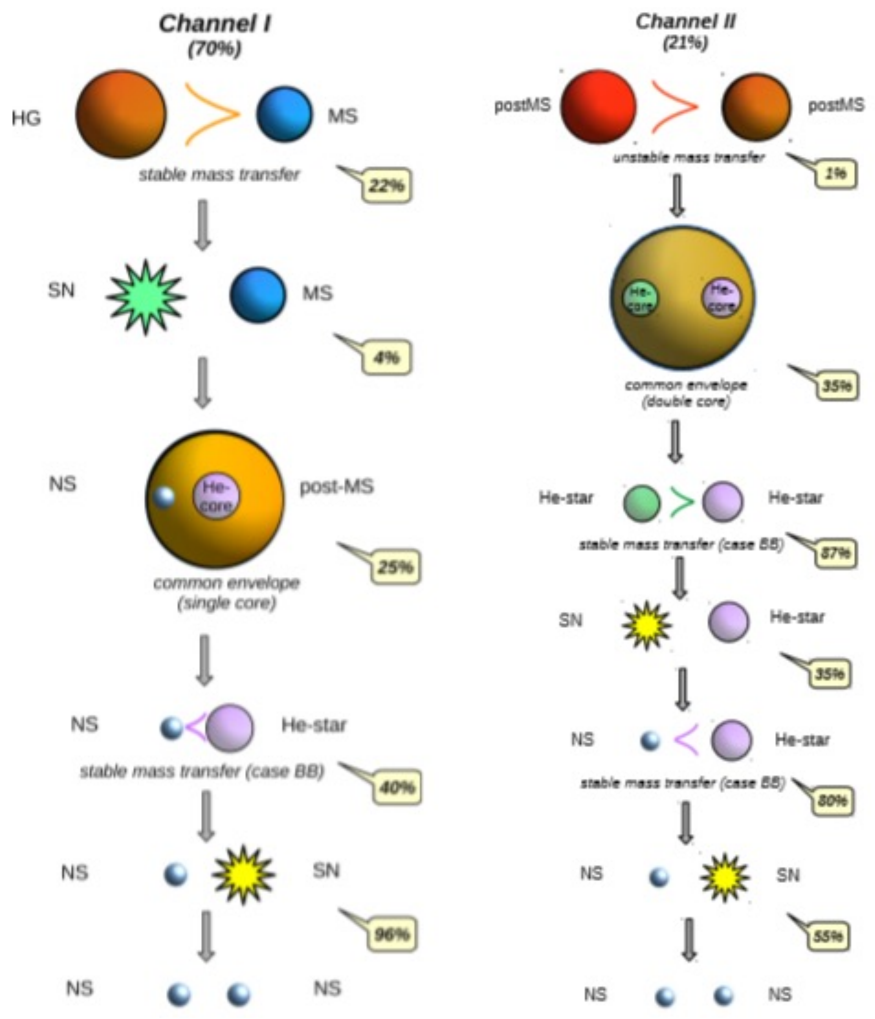

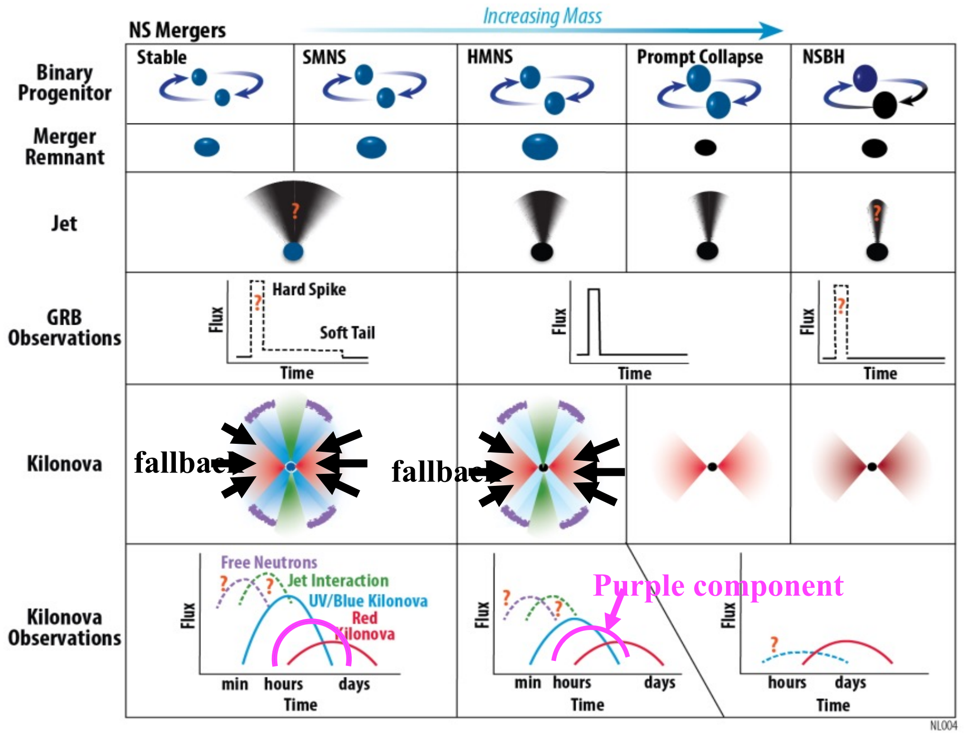

Multi-messenger observations of many BNS mergers and its EM counterparts (kilonova and sGRB) make it possible to:

- **constrain the formation and evolution of (binary) stars and lead to a deep understanding of stellar evolution;**
- **reveal the physical mechanisms in the strong field and extreme matter densities/magnetic fields that are responsible for kilonova and sGRB phenomena.**

Prospects

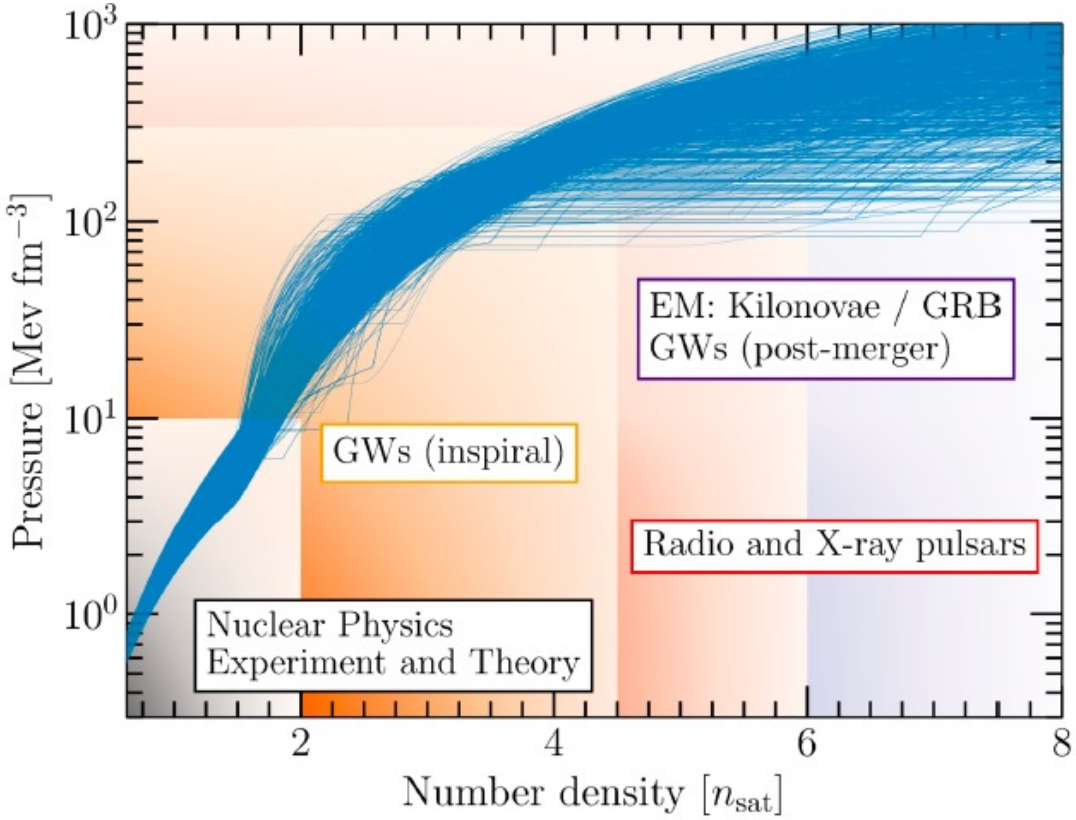

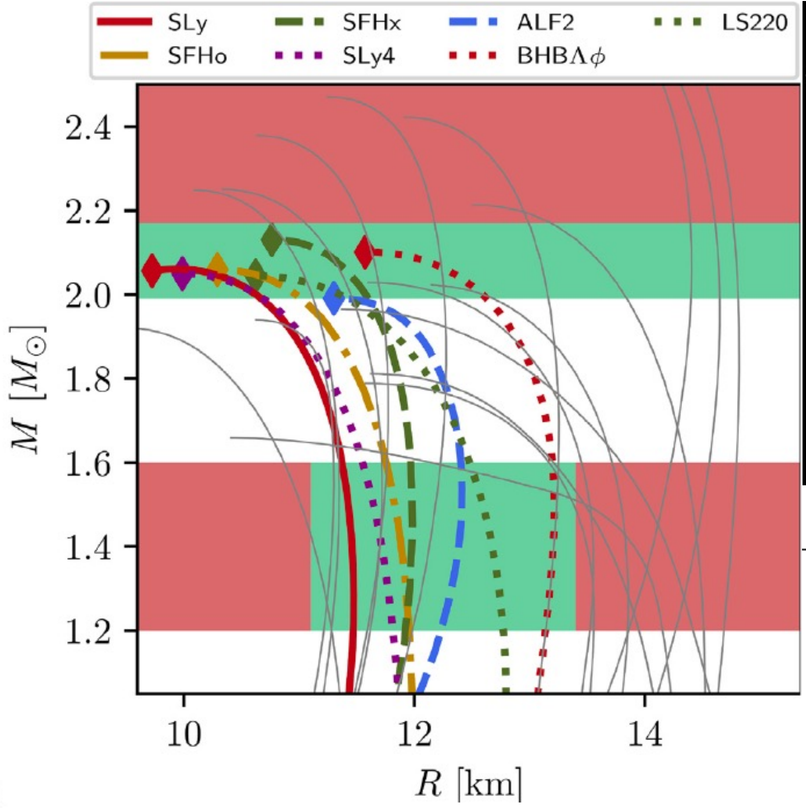

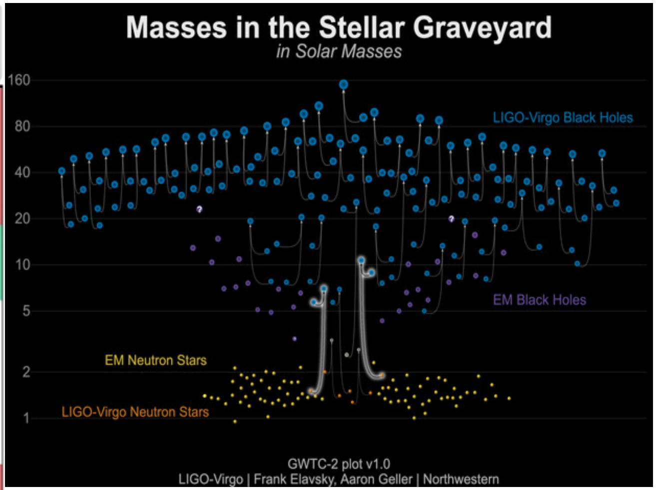

Reference	$R_{1.4M_\odot}$ [km]
Dietrich et al. [15]	$11.75^{+0.86}_{-0.81}$ (90%)
Essick et al. [51]	$12.54^{+0.71}_{-0.63}$ (90%)
Breschi et al. [23]	$11.99^{+0.82}_{-0.85}$ (90%)
Nicholl et al. [24]	$11.06^{+1.01}_{-0.98}$ (90%)
Raaijmakers et al. [25]	$12.18^{+0.56}_{-0.79}$ (95%)
Miller et al. [52]	$12.45^{+0.65}_{-0.65}$ (68%)
Huth et al. [16]	$12.01^{-0.78}_{-0.77}$ (90%)
this work [NMMA][53]	$11.98^{+0.35}_{-0.40}$ (90%)

Pang et al. arXiv:2205.08513
Coughlin et al. 2019, MNRAS

- **Tight constraint on the EOS of neutron stars;**
- **Witness the formation of event horizon.**

Prospects

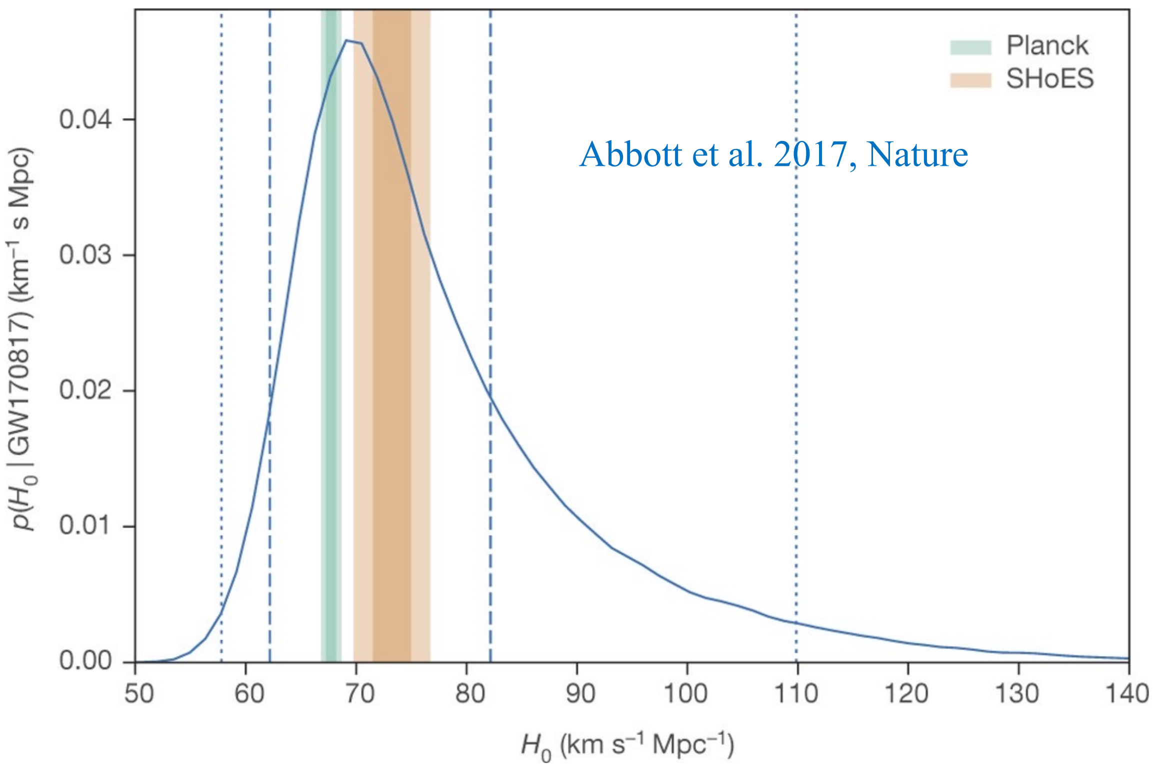

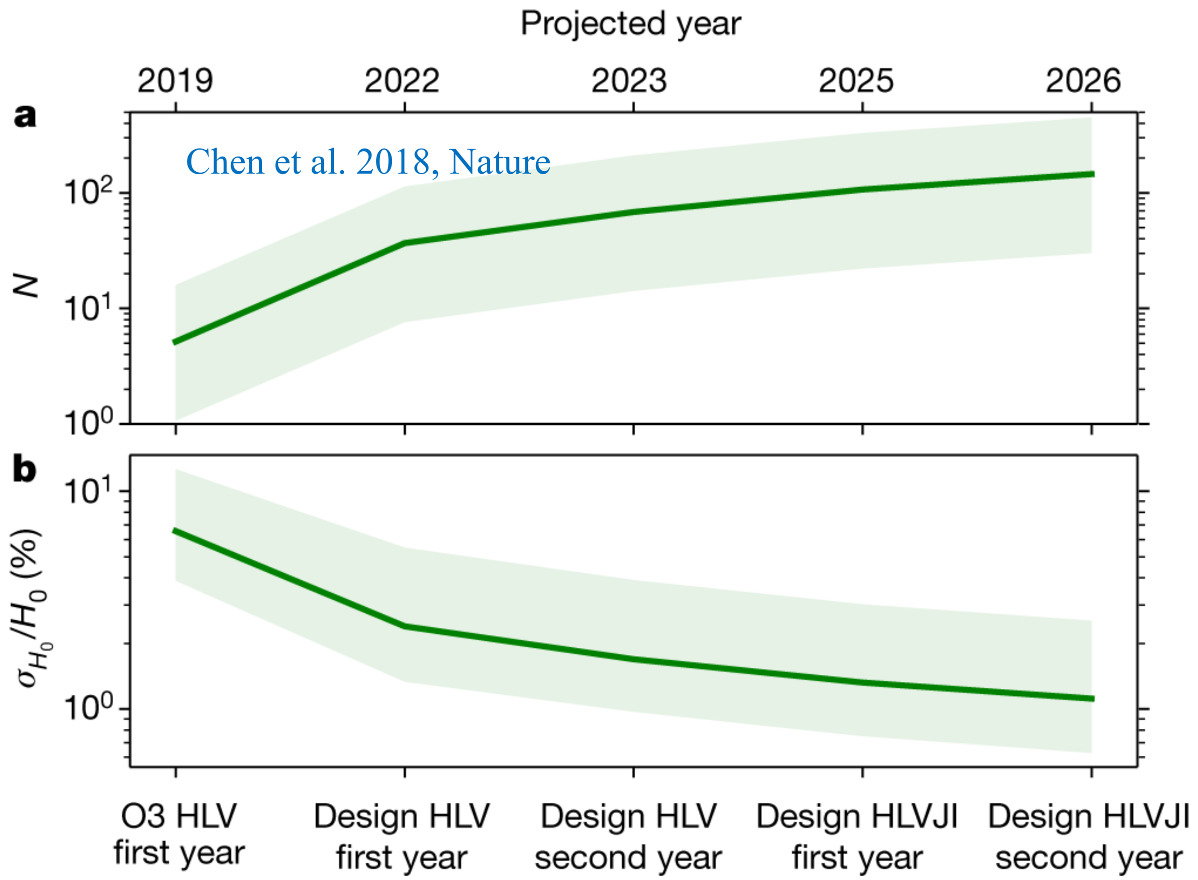

Cosmological applications as standard sirens to independently and accurately measure the Hubble constant and other cosmological parameters

Summary

- Present a comprehensive model for the formation and evolutoin of BNSs, reconstruct the distribution of Galactic BNSs and constrain the model parameters;
- Current GW observations of BNS mergers only put weak constraint on the CE evolution;
- Develop a phenomenological kilonova model by considering various procecsses, and explain the light curves of GW170817;
- Predict the luminosity function of kilonova;
- Predict the distribution of the properties of the kilonova host galaxies and find the predictions are well consistent with the observations on the host galaxies of short GRBs;
- Estimate the detection rate of lensed kilonovae.

Thank you for your attention!